Self#assembling amyloid#like peptides as exogenous second harmonic probes for bioimaging applications

Ni Ming (Orcid ID: 0000-0001-5284-2195)

Self-assembling amyloid-like peptides as exogenous second harmonic probes for bioimaging applications

Ming Ni [+]1,2, Shuangmu Zhuo [+]3, Ciprian Iliescu4,5, Peter T. C. So6,7, Jodhbir S. Mehta8, Hanry Yu1,6,9, Charlotte A. E. Hauser10

[1]Institute of Bioengineering and Nanotechnology, 31 Biopolis Way, The Nanos, Singapore 138669;
[2]School of Biological Sciences & Engineering, Yachay Tech University, Hacienda San José s/n, San Miguel de Urcuquí 100105, Ecuador
[3]Key Laboratory of Optoelectronic Science and Technology for Medicine of Ministry of Education, Fujian Normal University, Fuzhou, 350007, P. R. China
[4]BIGHEART, National University of Singapore, 14 Medical Drive, MD6, #14-01, 117597 Singapore
[5]Academy of Romanian Scientists, Splaiul Independentei nr. 54, Bucharest 050094, Romania
[6]Biosystems and Micromechanics IRG, Singapore-MIT Alliance for Research and Technology, 1 CREATE Way, #04-13/14 Enterprise Wing, 138602 Singapore;
[7]Department of Mechanical Engineering, Massachusetts Institute of Technology, 77 Massachusetts Avenue, Cambridge, MA 02139, USA
[8]Singapore Eye Institute and Singapore National Eye Center, 11 Third Hospital Avenue, 168751, Singapore
[9]Yong Loo Lin School of Medicine & Mechanobiology Institute, National University of Singapore, 14 Medical Drive, MD 9 #04-11, 117597, Singapore
[10]King Abdullah University of Science and Technology, Division of Biological & Environmental Science & Engineering, Laboratory for Nanomedicine, Al-Haytham Building (Bldg. 2), Office 4217, Thuwal 23955-6900, Kingdom of Saudi Arabia

[+] These authors contributed equally to this work.
* Corresponding Authors: M.N. (mingni.sg@gmail.com) or S.Z. (shuangmuzhuo@gmail.com) or H.Y. (hyu@ibn.a-star.edu.sg) or C.A.E.H. (charlotte.hauser@kaust.edu.sa).

This is the author manuscript accepted for publication and has undergone full peer review but has not been through the copyediting, typesetting, pagination and proofreading process, which may lead to differences between this version and the Version of Record. Please cite this article as doi: 10.1002/jbio.201900065

ABSTRACT

Amyloid-like peptides are an ideal model for the mechanistic study of amyloidosis, which may lead to many human diseases, such as Alzheimer's. The paper reports a strong second harmonic generation (SHG) effect of amyloid-like peptides, having a signal equivalent to or even higher than those of endogenous collagen fibers. Several amyloid-like peptides (both synthetic and natural) were examined under SHG microscopy and shown they are SHG-active. These peptides can also be observed inside cells (*in vitro*). This interesting property can make these amyloid-like peptides second harmonic probes for bioimaging applications. Furthermore, SHG microscopy can provide a simple and label-free approach to detect amyloidosis. Lattice corneal dystrophy was chosen as a model disease of amyloidosis. Morphological difference between normal and diseased human corneal biopsy samples can be easily recognized, proving that SHG can be a useful tool for disease diagnosis.

Keywords: bioimaging, non-linear optical materials, second harmonic generation, self-assembly, ultrashort peptides.

1. Introduction

Amyloid-like peptides are responsible for amyloidosis which is an important feature for several human diseases, including Alzheimer (AD) [1-2], Parkinson [3], type II diabetes [4], cataracts [5], or lattice corneal dystrophy (LCD) [6]. The inhibition of amyloid-like peptides production is a promising strategy for the development of therapeutic agents to treat such diseases. However, the mechanism of amyloidosis is still unclear. One logical mechanistic approach is to study how these amyloid-like peptides/proteins fold or misfold [2, 7]. In this direction, ultrashort peptides (having only three to seven amino acids) provide us an ideal model for mechanistic studies. For example, GGVVIA (GA_6) and KLVFFAE (KE_7), can self-assemble into amyloid-like aggregates [8-9]. The previously mentioned peptides are also known as the core sequence of amyloid-β (A_β). A_β is the major component in the amyloid aggregates responsible for AD. Besides ultrashort peptides that can be found in natural peptides/proteins, several designed synthetic ultrashort peptides, such as IVD (ID_3) and LIVAGD (LD_6), have shown similar behavior [9-10]. Both the natural and synthetic peptides are amyloid-like peptides. Ultrashort amyloid-like peptides can not only be useful for screening of amyloid inhibitors [10-11], but also as a new type of biomaterials with desirable properties such as biocompatibility and biological activities [8-9, 12-13]. They all form cross-β peptide structure at a molecular level. Mechanically they are rigid, with strength comparable to steel [14]. Morphologically they are helical fibers of micrometers in length but only 7-10 nm in diameter [15], having a similar morphology to collagen fibers [10, 16]. Supramolecular assemblies of collagen in tissues have been visualized by SHG microscopy [17]. In particular,

collagen I and collagen II have been proven to efficiently produce SHG signals [17-18]. SHG has been applied to investigate rat and human corneal samples [19-22]. Collagen fibrils in cornea were observed under SHG microscopy without any labelling. The orientation, morphology and submicron heterogeneity of collagen fibers were quantitatively analyzed by SHG, which potentially can be used for in vivo diagnosis of corneal diseases, such as LCD. Besides collagen is used as a biomarker for LCD, extracellular deposition of amyloid β within cornea is commonly thought as the main reason for LCD.

Inspired by these findings, we demonstrate here the non-linear optical (NLO) properties of self-assembled ultrashort amyloid-like peptides [23] and explore their potentials as novel organic probes for SHG imaging. Besides significant advantages over the conventional fluorescence imaging techniques such as deeper optical penetration, lower photo-damage and longer observation time [24-27], SHG microscopy provides a simple and label-free approach to detect amyloid-like peptides, which can be a useful tool for disease diagnosis, especially for LCD.

2. Materials and Methods

2.1 Ultrashort Amyloid-Like Peptides

Amyloid-like peptides were purchased from the American Peptide Company (purity ≥95%). The peptide sequences were confirmed by liquid chromatography-mass spectrometry (LC-MS). Net peptide content varied between 70% and 85%. All

peptides were acetylated at the N terminus. Peptide handling and hydrogel preparation were done as reported previously [10, 28].

2.2 Peptide Particles

The preparation of the peptide particles was performed by hydrodynamic focusing, method described in previous work [29-31]. The particle size was determined by scanning electron microscopy, showing a grain size of around 5 μm.

2.3 Cell Culture

Both HeLa and human dermal fibroblasts were cultured in DMEM supplemented with 10% fetal bovine serum and 1% penicillin/streptomycin (Life Technologies, Singapore).

2.4 Human corneal biopsy samples

The human corneal biopsy samples were provided by Singapore General Hospital. The normal tissue was from a seventy-eight year-old Caucasian male. The diseased tissue was from a sixty-year-old female who has lattice corneal dystrophy (LCD). The study was approved by the institutional review board (IRB) from Singhealth.

2.5 SHG Imaging

SHG images were acquired using a commercial laser scanning microscopic imaging system (Zeiss LSM 510 META, Jena, Germany) coupled to a mode-locked femtosecond Ti: sapphire laser (Mai-Tai broadband, Spectra-Physics), tunable from 710 nm to 990 nm. To achieve spectral analysis and detect the SHG signal, we used the META detector with 32-gated photon counting module [17].

3 Results and Discussions

3.1 A hexamer peptide is collagen-like and SHG-active

To test whether these amyloid-like peptides are SHG-active, we first investigated a hexamer peptide, Ac-LIVAGK-NH_2, (LK_6). Peptide powder was dissolved in pure water and peptide microparticles were assembled on a microfluidic chip using hydrodynamic focusing techniques. The resulting peptide microparicles were examined under SHG microscopy. During the whole experiments, only the backscattered geometry was employed because it is the only suitable configuration for *in vivo* imaging [26]. We chose collagen I as a control, being shown that SHG microscopy can visualize supramolecular assembly of collagen in tissues [26]. Both collagen I and peptide particles showed SHG signals with comparable intensity. This is shown in **Figure 1a** where the SHG signal from the collagen fibers of a rat liver tissue was compared with the signal from LK_6 peptide particles (instrument settings for both SHG imaging being the same). The fine structures of collagen and peptide particles can be clearly seen under SHG and SEM- **Figure 1b and c**. Moreover, LK_6 peptide exhibits typical SHG characteristics. Excited at 810 nm, LK_6 emitted a sharp SHG peak at 405 nm (**Figure 1d**). This is a main characteristic of SHG: two photons can be converted into one photon at exactly half of the wavelength. We then examined the excitation wavelength tunability of SHG signals from LK_6 peptide. In **Figure 1e**, as the excitation wavelength was increased from 810 to 890 nm, the wavelength of the SHG signals from the LK_6 peptide particles increased from 405 to 445 nm respectively. The opportunity of tuning the excitation wavelength gives the advantage of best matching with the optical properties of the sample. It is known that

a biological sample (cells/tissues) presents auto-fluorescence. It should be noted that the SHG emission is significantly enhanced when exciting with a quasi-resonant scheme (~720 nm maximum). However, longer wavelengths will result in greater depth of penetration because of reduced scattering and also avoid auto-fluorescent absorption bands in tissues. In this work, we used excitation wavelength ranging from 810 to 890 nm, which falls in the so called ¨therapeutic window¨ or ¨optical window¨. The common problems encounter by conventional fluorescent microscopy are circumvented. In addition, a further increase of the penetration depth in tissues can be achieved by simply increasing excitation wavelength. **Figure 1f** showed the emission wavelength data of the SHG signal (λ_{ex} = 850 nm). The data in the graph was fitted to a Gaussian curve exhibiting a maximum at 425nm, which is exactly half the excitation wavelength of 850 nm. The bandwidth (full width at half-maximum of Gaussian distribution, FWHM) was narrow (~10 nm) and it obeyed a $1/\sqrt{2}$ relationship to the corresponding wavelength profile of the fundamental beam (~15 nm). Moreover, the dependence of the output signal on irradiation intensity was measured by varying the 850nm excitation intensity. The linear regression, applied to the log-log plots (**Equation 1**), revealed a quadratic power dependence of SHG intensity to power intensity, as shown in the **Figure 1g**.

$$\log[I_{425}] = 0.45 + 2.01 \times \log[I_{850}] \quad (1)$$

The intensity of SHG signal is proportional to the square of the incident laser intensity. This confirmed the two-photon nature of the emission from LK_6 peptide.

3.2 Cytocompatibility of a hexamer peptide

In order to use LK_6 for bioimaging applications, such as *in vitro* cells monitoring or *in vivo* imaging, we assessed the cytotoxicity of LK_6 using MTS test and live/dead assay with two human cell lines, human epithelial carcinoma cells (HeLa) and primary human dermal fibroblasts (HDF) (**Figure 2**). Cells were exposed to cell culture media containing different concentrations of LK_6 solution (0.1 to 1000 μg/mL) and incubated for 48 h. Cell viability at various LK_6 concentrations was either equivalent to or even higher than that of untreated cells over the whole concentration range which was tested in this study (**Figure 2a)**. To further confirm these results, we stained cells with or without peptide exposure using solutions containing a mixture of calcein AM and ethidium homodimer-1 (EthD-1). Calcein AM can penetrate cell membrane and be converted within the cell to membrane impermeable green fluorescent calcein, while red fluorescent EthD-1 is unable to permeate the intact cell membrane of living cells. **Figure 2 b** shows the representative live/dead images of cells in response to LK_6 solutions (1 and 1000 μg/mL). LK_6 displayed no toxicity to both HDF and HeLa cells, in agreement with the results of the MTS assays.

3.3 Comparison of synthetic and natural amyloid-like peptides under SHG microscopy

Several other amyloid-like peptides, including both natural amyloidogenic core sequences (NL_6, DF_5, GA_6, and KE_7) and designed synthetic peptides (LD_6, IS_6 and IK_3) were examined under SHG excitation. The peptide sequences are listed in Table

1. All these peptides are SHG-active. We used a powder technique developed by Kurtz and Perry [32] to evaluate the SHG efficiency of these second-order nonlinear optical materials. Sucrose was chosen as control to evaluate SHG efficiencies [33]. In Table 1, all tested amyloid-like peptides showed higher or equivalent SHG efficiency compared to sucrose. These can be explained through their molecular structures. LD_6 is known to form hydrogel at much lower concentrations compared to LK_6. The trimer IK_3 has larger dipole moment compared to LK_6. Human collagen subtypes I to V were also examined (**Table 1**) for their SHG activity. Only Collagen type I and II showed positive results, aspect that is in concordance with the previous findings reported in the literature [18, 34]. Moreover, some amyloid-like peptides such as IVK, LIVAGD or even ILVAGS showed even higher SHG efficiency than collagen subtypes (I and II). This suggests the opportunity of using these materials as SHG probes.

The investigation of the SHG efficiency for four natural amyloidogenic core sequences indicates the following order: KE_7 > GA_6 > DF_5 > NL_6 (**Table 1 and Figure 3**). KE_7 (KLVFFAE), containing its diphenylalanine (FF) motif, showed the highest SHG efficiency among these four peptides. However, its SHG efficiency is similar as that of IK_3. It is noteworthy that IK_3 is an aliphatic peptide. Aromatic residues such as tyrosine and tryptophan are known to be used as an endogenous molecular probe of peptides and proteins for SHG at the air-water interface [35]. However, our results indicated that aromatic residues are not necessary for higher SHG efficiency. LD_6, IS_6, LK_6 and IK_3 are all aliphatic and lacking aromatic residues,

clearly makes them a unique type of peptides for SHG applications. These peptides are amphiphilic [10, 16], consisting of an aliphatic amino acid tail of decreasing hydrophobicity and a hydrophilic head. They can self-assembly via parallel-antiparallel α-helical pairs and subsequent stacking into β-turn fibrils, which show striking similarity to collagen fibers [16]. We reasoned that the origin of these amyloid-like peptides' SHG activity comes from their nanostructures. A recent study showed that the origin of SHG signals from collagen fibers possibly lies in their peptide bonds [36]. The collagen fiber building blocks were mimicked by tri-amino acid peptides PPG and GGG (P and G are the one letter code for Proline and Glycine respectively).

3.4 A hexamer peptide as a second harmonic probe for in vitro cell imaging

Another possible application for LK_6 is to use it for high-resolution cell imaging. To this end, HeLa cells were incubated with biotin-conjugated LK_6 for 4 h and then fixed for immune staining. LK_6 peptides were visualized by both SHG and confocal fluorescence microscopy. In **Figure 4**, biotin-conjugated peptides displayed green color when DyLight™ 488-conjugated NeutrAvidin™ (Thermo Scientific, Singapore, Prod #: 22832) was added. Meanwhile, amyloid-like peptides displayed pseudo red color under SHG. These results revealed two interesting features of the investigated amyloid-like peptides: 1) they can be visualized under SHG without any label; 2) they can be up-taken by cells. We want to point out that when attaching additional labels such as chromophores to the amyloid-like peptide structure for bioimaging purposes,

it may easily change the molecular properties of the native peptide molecules. Thus, additional changes of the peptide molecule are time consuming and asking for more costly synthetic approaches. Hence, using amyloid-like peptides in their native structure for a label-free SHG bioimaging technology could certainly be useful as an attractive and minimal-invasive diagnostic tool.

In addition, a molecular-level property of the nonlinearity, i.e., the first hyperpolarizability, β, was measured by Hyper Rayleigh Scattering (HRS). The first hyperpolarizability of these trimers was about 0.087×10^{-30} esu [36]. However, the first hyperpolarizability of collagen I was found to be $(1250 \pm 20) \times 10^{-30}$ esu [36], which could be viewed as ten thousand trimers combining together. In terms of SHG signals, collagen consists a triple helix structure, which shows very strong SHG signals. Single collagen amino acid such as glycine, proline and hydroproline does not show SHG signals as strong as collagen fibrils. We hypothesize that the aggregation of these tripeptides gives the much stronger SHG signals in comparison with isolated tripeptides. Based on the non-linearity of the intrinsic peptide bonds and their aggregation capability, these amyloid-like peptides can generate SHG signals, just like collagen.

3.5 Diseased and normal human corneal biopsy samples examined by SHG microscopy

More interestingly, when we examined the human corneal biopsy samples (**Figure 5a and 5b**), both amyloids (indicated by arrow) and collagen can be seen. The human

corneal biopsy samples were provided by Singapore General Hospital. The normal tissue was from a seventy-eight year-old Caucasian male. The diseased tissue was from a sixty-year-old female who has lattice corneal dystrophy (LCD). Under SHG, the normal corneal sample showed collagen fibrils aligned as parallel straight lines in stroma. By contrast diseased samples showed collagen fibrils became curved and thicker. The thickened collagen fibrils could be due to amyloid deposits [37]. Thus, SHG provides us a new diagnostic tool for lattice corneal dystrophy (LCD) that is superior to the existing histological staining methods: SHG being a label-free method.

4. Conclusions

We demonstrated that amyloid-like peptides are nonlinear optical materials showing strong SHG signals and a quadratical dependence of SHG intensity to power intensity. Amyloid-like peptides show no cytotoxic effect to human cells and can be observed inside cells without fluorescent labelling, which make them suitable as second harmonic probes. Amyloid-like peptide nanomaterials hold great potential in nanotechnology and nanomedicine. We assembled amyloid peptide microparticles via hydrodynamic focusing on a microfluidic chip. We could encapsulate small molecule drugs, DNA or RNA when we assembled them on chip. Their nonlinear optical properties hold promise for new bioimaging applications. The development of SHG microendoscopy [38] could open more opportunities for using amyloid-like peptides as a SHG probe for more bioimaging applications. The imaging capability in combination with therapeutic capability via drug encapsulation will make these amyloid-like peptides interesting theranostic agents.

Acknowledgements

This work was funded by the Institute of Bioengineering and Nanotechnology (Biomedical Research Council, Agency for Science, Technology and Research, Singapore). S.Z. thanks the SMART Scholars Programme, the National Natural Science Foundation of China (81771881), the Natural Science Foundation of Fujian Province (2018J07004), the Special Funds of the Central Government Guiding Local Science and Technology Development (2017L3009) for financial support.

Author Information: The authors declare no competing financial interests.

References

[1] Soto C, Brañes MC, Alvarez J, Inestrosa NC. Structural Determinants of the Alzheimer's Amyloid β-Peptide. J. Neurochem. 1994; 63: 1191-8.
[2] Chiti F, Dobson CM. Protein Misfolding, Functional Amyloid, And Human Disease. Annu. Rev. Biochem. 2006; 75: 333-66.
[3] Polymeropoulos MH, Lavedan C, Leroy E, Ide SE, Dehejia A, Dutra A, Pike B, Root H, Rubenstein J, Boyer R. Mutation In The A-Synuclein Gene Identified In Families With Parkinson's Disease. Science 1997; 276: 2045-7.
[4] Clark A, Lewis C, Willis A, Cooper G, Morris J, Reid K, Turner R. Islet Amyloid Formed From Diabetes-Associated Peptide May Be Pathogenic In Type-2 Diabetes. Lancet 1987; 330: 231-4.
[5] Goldstein LE, Muffat JA, Cherny RA, Moir RD, Ericsson MH, Huang X, Mavros C, Coccia JA, Faget KY, Fitch KA. Cytosolic B-Amyloid Deposition And Supranuclear Cataracts In Lenses From People With Alzheimer's Disease. Lancet 2003; 361: 1258-65.
[6] Gorevic PD, Munoz PC, Gorgone G, Purcell JJ, Rodrigues M, Ghiso J, Levy E, Haltia M, Frangione B. Amyloidosis Due To A Mutation Of The Gelsolin Gene In An American Family With Lattice Corneal Dystrophy Type II. N. Eng. J. Medicine 1991; 325: 1780-5.
[7] Dobson CM. Protein Folding And Misfolding. Nature 2003; 426: 884-90.
[8] Kirschner DA, Inouye H, Duffy LK, Sinclair A, Lind M, Selkoe DJ. Synthetic Peptide Homologous To Beta Protein From Alzheimer Disease Forms Amyloid-Like Fibrils In Vitro. P. Natl. Acad. Sci. USA 1987; 84: 6953-7.
[9] Hauser CA, Maurer-Stroh S, Martins IC. Amyloid-Based Nanosensors And Nanodevices. Chem. Soc. Rev. 2014; 43: 5326-45.
[10] Hauser CA, Deng R, Mishra A, Loo Y, Khoe U, Zhuang F, Cheong DW, Accardo A, Sullivan MB, Riekel C. Natural Tri-To Hexapeptides Self-Assemble In Water To Amyloid B-Type Fiber Aggregates By Unexpected A-Helical Intermediate Structures. P. Natl. Acad. Sci. USA 2011; 108: 1361-6.
[11] Azriel R, Gazit E. Analysis Of The Minimal Amyloid-Forming Fragment Of The Islet Amyloid Polypeptide An Experimental Support For The Key Role Of The Phenylalanine Residue In Amyloid Formation. J. Biol. Chem. 2001; 276: 34156-61.
[12] Ni M, Zhuo S. Applications of self-assembling ultrashort peptides in bionanotechnology. RSC Adv. 2019; 9: 844-52.
[13] Cherny I, Gazit E. Amyloids: not only pathological agents but also ordered nanomaterials. Angew. Chem. Int. Edit. 2008; 47: 4062-9.
[14] Smith JF, Knowles TP, Dobson CM, MacPhee CE, Welland ME. Characterization Of The Nanoscale Properties Of Individual Amyloid Fibrils. P. Natl. Acad. Sci. USA 2006; 103:15806-11.
[15] Shirahama T, Cohen AS. High-Resolution Electron Microscopic Analysis Of The Amyloid Fibril. J. Cell. Biol. 1967; 33: 679-708.
[16] Mishra A, Loo Y, Deng R, Chuah YJ, Hee HT, Ying JY, Hauser CA. Ultrasmall Natural Peptides Self-Assemble To Strong Temperature-Resistant Helical Fibers In Scaffolds Suitable For Tissue Engineering. Nano Today 2011; 6: 232-9.

[17] Zhuo S, Chen J, Wu G, Xie S, Zheng L, Jiang X, Zhu X. Quantitatively Linking Collagen Alteration And Epithelial Tumor Progression By Second Harmonic Generation Microscopy. Appl. Phys. Lett. 2010; 96: 213704.
[18] Chen X, Nadiarynkh O, Plotnikov S, Campagnola PJ. Second Harmonic Generation Microscopy For Quantitative Analysis Of Collagen Fibrillar Structure. Nat. Protoc. 2012; 7: 654-69.
[19] Latour G, Gusachenko I, Kowalczuk L, Lamarre I, Schanne-Klein MC. In vivo structural imaging of the cornea by polarization-resolved second harmonic microscopy. Biomed. Opt. Express 2012; 3: 1-15.
[20] Bancelin S, Aime C, Gusachenko I, Kowalczuk L, Latour G, Coradin G, Schanne-Klein MC, Determination of collagen fibril size via absolute measurements of second-harmonic generation signals. Nat. Commun. 2014; 5: 4920.
[21] Mercatelli R, Ratto F, Rossi F, Tatini F, Menabuoni L, Malandrini A, Nicoletti R, Pini R, Pavone FS, Cicchi RR. Three-dimensional mapping of the orientation of collagen corneal lamellae in healthy and keratoconic human corneas using SHG microscopy. J. Biophoton. 2017; 10: 75-83.
[22] Mercatelli R, Mattana S, Capozzol Li, Ratto F, Rossi F, Pini R, Fioretto D, Pavone FS, Caponi S, Cicchi R. Morpho-mechanics of human collagen superstructures revealed by all-optical correlative micro-spectroscopies. Communications Biology 2019; 2: 117.
[23] Franken PA, Hill AE, Peters CE, Weinreich G. Generation Of Optical Harmonics. Phys. Rev. Lett., 1961; 7: 118-9.
[24] Zipfel WR, Williams RM, Christie R, Nikitin AY, Hyman BT, Webb WW. Live Tissue Intrinsic Emission Microscopy Using Multiphoton-Excited Native Fluorescence And Second Harmonic Generation. P. Natl. Acad. Sci. USA 2003; 100: 7075-80.
[25] Pantazis P, Maloney J, Wu D, Fraser SE. Second Harmonic Generating (SHG) Nanoprobes For In Vivo Imaging. P. Natl. Acad. Sci. USA 2010; 107: 14535-40.
[26] Campagnola PJ, Loew LM. Second-harmonic imaging microscopy for visualizing biomolecular arrays in cells, tissues and organisms. Nat. Biotech. 2003; 21: 1356-60.
[27] Yu F, Zhuo S, Qu Y, Choudhury D, Wang Z, Iliescu C, Yu H. On Chip Two-Photon Metabolic Imaging For Drug Toxicity Testing. Biomicrofluidics 2017; 11: 034108.
[28] Chan KH, Lee WH, Ni M, Loo Y, Hauser CAE. C-Terminal Residue of Ultrashort Peptides Impacts on Molecular Self-Assembly, Hydrogelation, and Interaction with Small-Molecule Drugs. Sci. Rep. 2018; 8: 17127.
[29] Ni M, Tresset G, Iliescu C. Self-Assembled Polysulfone Nanoparticles Using Microfluidic Chip. Sensor. Actuat. B-Chem. 2017; 252: 458-62.
[30] Iliescu C, Tresset G. Microfluidics-Driven Strategy for Size-Controlled DNA Compaction by Slow Diffusion through Water Stream. Chem. Mater. 2015; 27: 8193-7.
[31] Tresset G, Marculescu C, Salonen A, Ni M, Iliescu C. Fine Control Over The Size Of Surfactant–Polyelectrolyte Nanoparticles By Hydrodynamic Flow Focusing. Anal. Chem., 2013; 85: 5850-6.
[32] Kurtz S, Perry T. A Powder Technique For The Evaluation Of Nonlinear Optical Materials. J. Appl. Phys., 1968; 39: 3798-813.

[33] Bourhill G, Mansour K, Perry KJ, Khundkar L, Sleva ET, Kern R, Perry JW, Williams ID, Kurtz SK. Powder Second Harmonic Generation Efficiencies Of Saccharide Materials. Chem. Mater. 1993; 5: 802-8.
[34] Su PJ, Chen WL, Li TH, Chou CK, Chen TH, Ho YY, Huang CH, Chang SJ, Huang YY, Lee HS. The Discrimination Of Type I And Type II Collagen And The Label-Free Imaging Of Engineered Cartilage Tissue. Biomaterials 2010; 31: 9415-21.
[35] Nasir MN, Benichou E, Loison C, Russier-Antoine I, Besson F, Brevet PF. Influence Of The Tyrosine Environment On The Second Harmonic Generation Of Iturinic Antimicrobial Lipopeptides At The Air–Water Interface. Phys. Chem. Chem. Phys., 2013; 15: 19919-24.
[36] Duboisset J, Deniset-Besseau A, Benichou E, Russier-Antoine I, Lascoux N, Jonin C, Hache F, Schanne-Klein MC, Brevet PF. A Bottom-Up Approach To Build The Hyperpolarizability Of Peptides And Proteins From Their Amino Acids. J. Phys. Chem. B 2013; 117: 9877-81.
[37] Anandalakshmi V, Murugan E, Leng EGT, Ting LW, Chaurasia SS, Yamazaki T, Nagashima T, George BL, Peh GSL, Pervushin K, Lakshminarayanan R, Mehta JS. Effect of position-specific single-point mutations and biophysical characterization of amyloidogenic peptide fragments identified from lattice corneal dystrophy patients. Biochem J. 2017; 474:1705-25.
[38] Zhang Y, Akins ML, Murari K, Xi J, Li MJ, Luby-Phelps K, Mahendroo M, Li X. A Compact Fiber-Optic SHG Scanning Endomicroscope And Its Application To Visualize Cervical Remodeling During Pregnancy. P. Natl. Acad. Sci. USA 2012; 109: 12878-83.

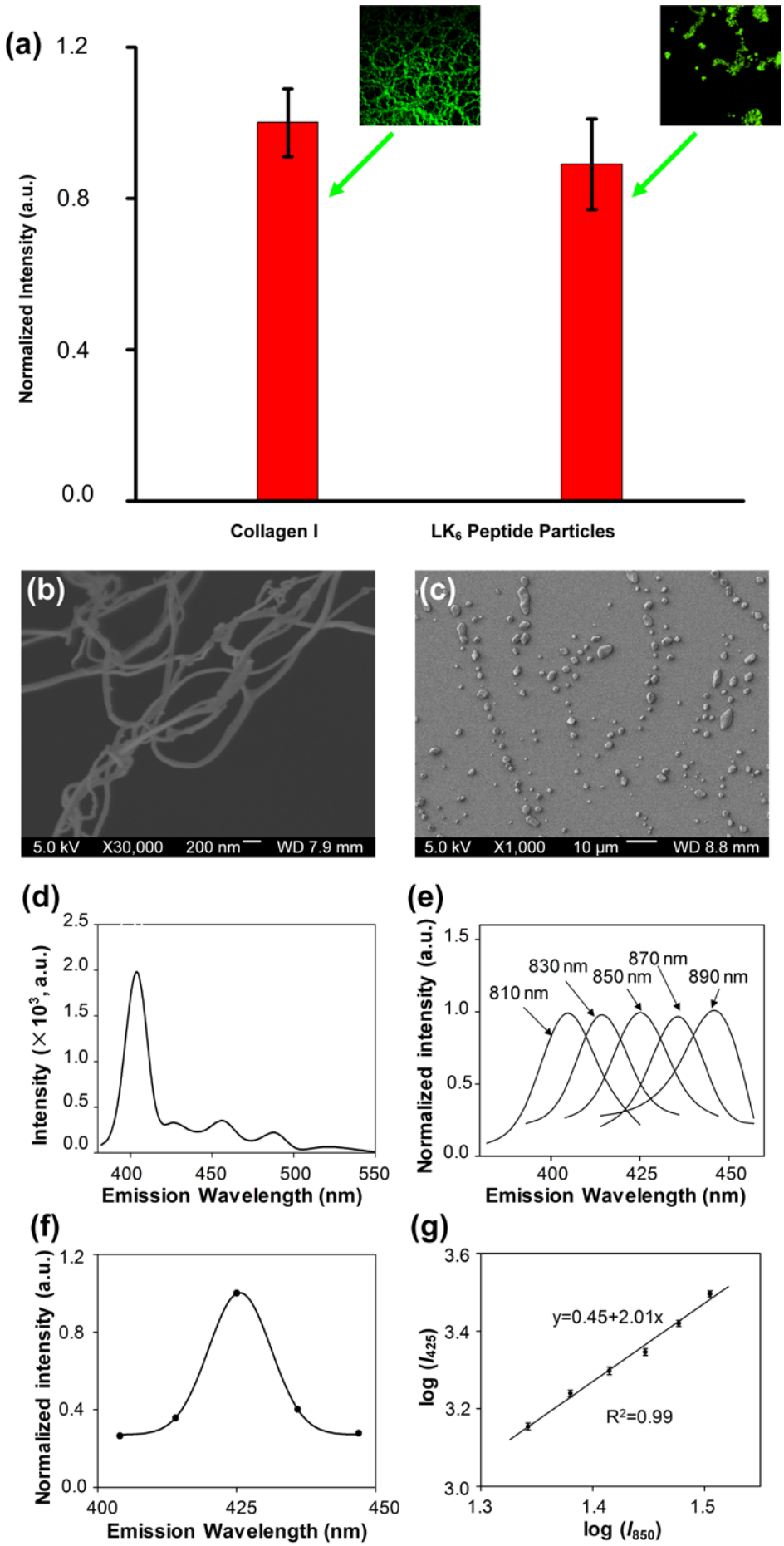

Figure 1. (a) Comparison of the SHG signal intensity from endogenous collagen I to LK6 peptide particles. Five spots from each image were chosen and the SHG signal intensity was normalized to collagen I (mean ± standard deviation, n=5); (b) SEM image of collagen fibers; (c) SEM image peptide particles. d) SHG signal spectrum of LK_6 peptide. Signal was ranging from 380 to 550 nm with excitation wavelength of 810 nm and peak emission wavelength was shown at 405 nm; (e) Spectral peaks at various excitation wavelengths spanning a broad spectral region (810-890 nm); (f) Emission λ-scan of the SHG signal (λ_{ex} = 850 nm) acquired from SHG imaging of LK_6 peptide particles. The solid spheres represent back scattering SHG data and the solid line represents a Gaussian fit. The full width at half-maximum of the fitted curve bears a $1/\sqrt{2}$ relation to the spectral profile of the corresponding beam; (g) Log-log plot of the above SHG signal measurements demonstrating a log[I425] = 0.45 + 2.01 × log[I850] dependence, quadratic to a good approximation, consistent with nonlinear second order optical upconversion.

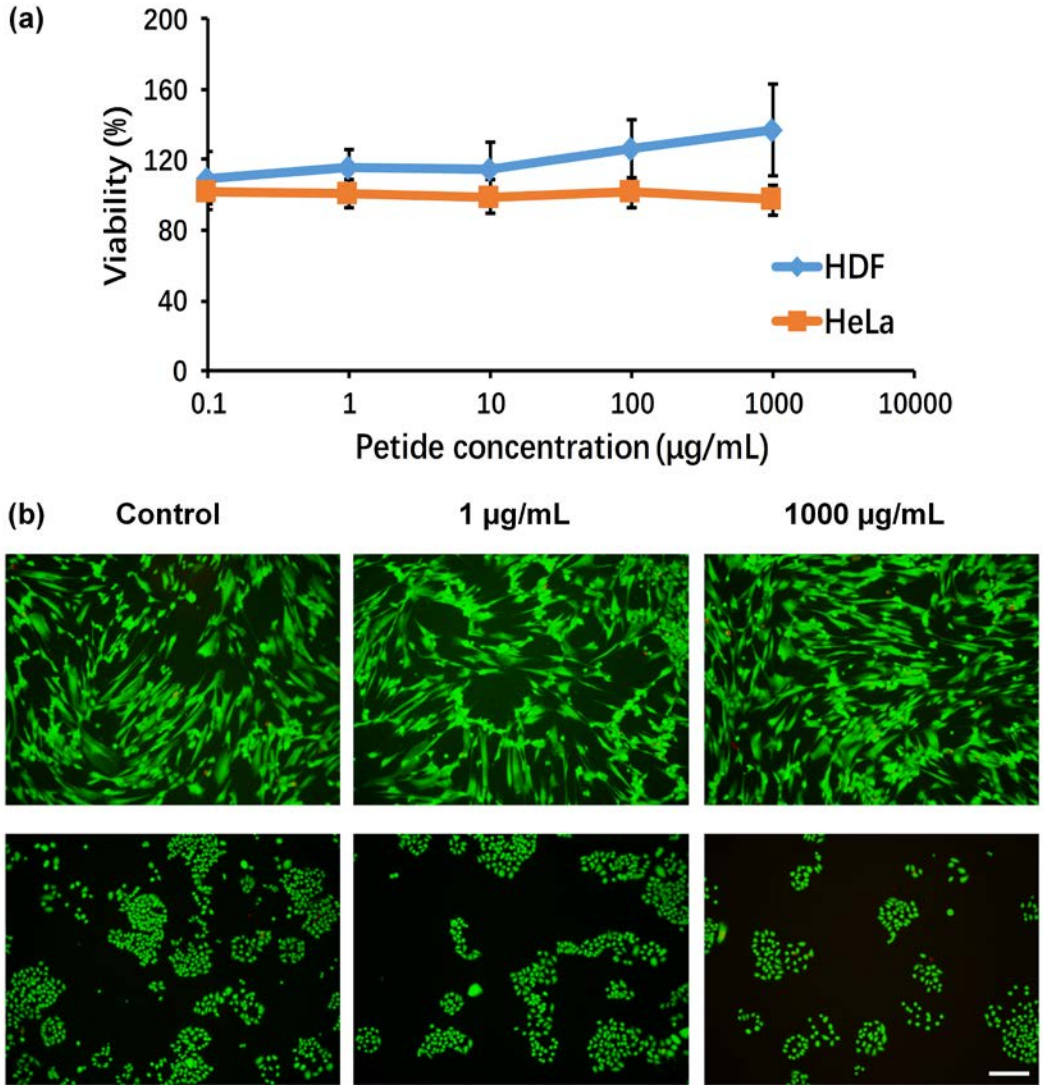

Figure 2. Cytotoxicity studies of LK6 peptide treated HDF and HeLa cells. (a) Cell viability at 48 h of HDF and HeLa cells incubated with cell culture media containing LK_6 peptide solutions, as determined using MTS assay (mean ± standard deviation, n=9). Concentrations ranged from 0.1 to 1000 μg/mL. (b) Cytotoxicity determined by Calcein AM/EthD-1 (live/dead, green/red) staining method after 48 h treated with 1 and 1000 μg/mL LK_6 peptide solutions using non-treated cells as control. Scale bar: 100 μm.

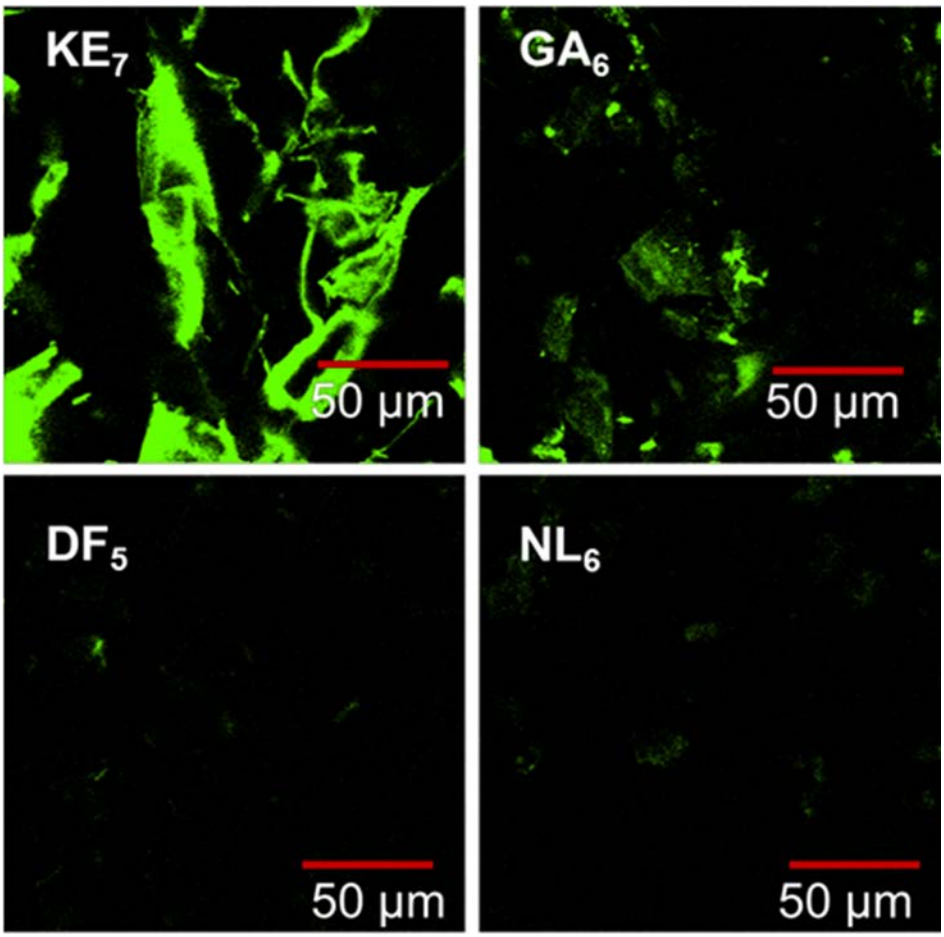

Figure 3. SHG images of four pristine peptides with natural amyloidogenic core sequences. The whole window was covered with pristine peptides. However, only part of the peptides can be visualized under SHG microscopy. The SHG intensity follows the order of KE7 > GA6 > DF5 > NL6. Scale bars: 50 μm.

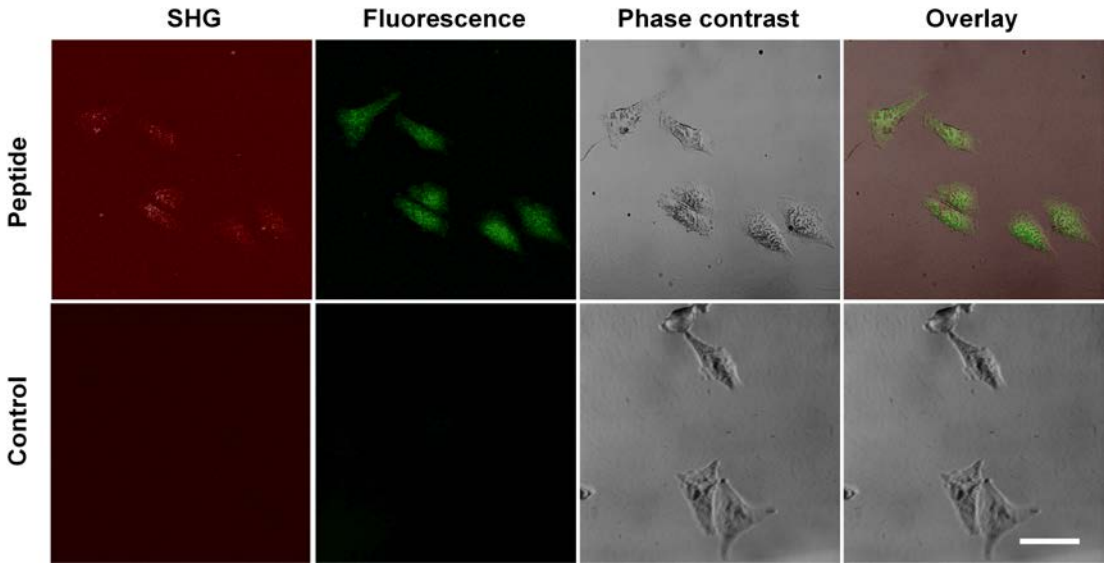

Figure 4. Cellular uptake of biotin-conjugated LK_6. Upper panel: HeLa cells exposed to biotin-conjugated LK_6 peptide containing medium. Peptides in HeLa cells displayed pseudo red color (SHG) and green color (fluorescence). Lower panel: HeLa cells exposed to normal medium without peptide (control). Scale bar: 50 μm

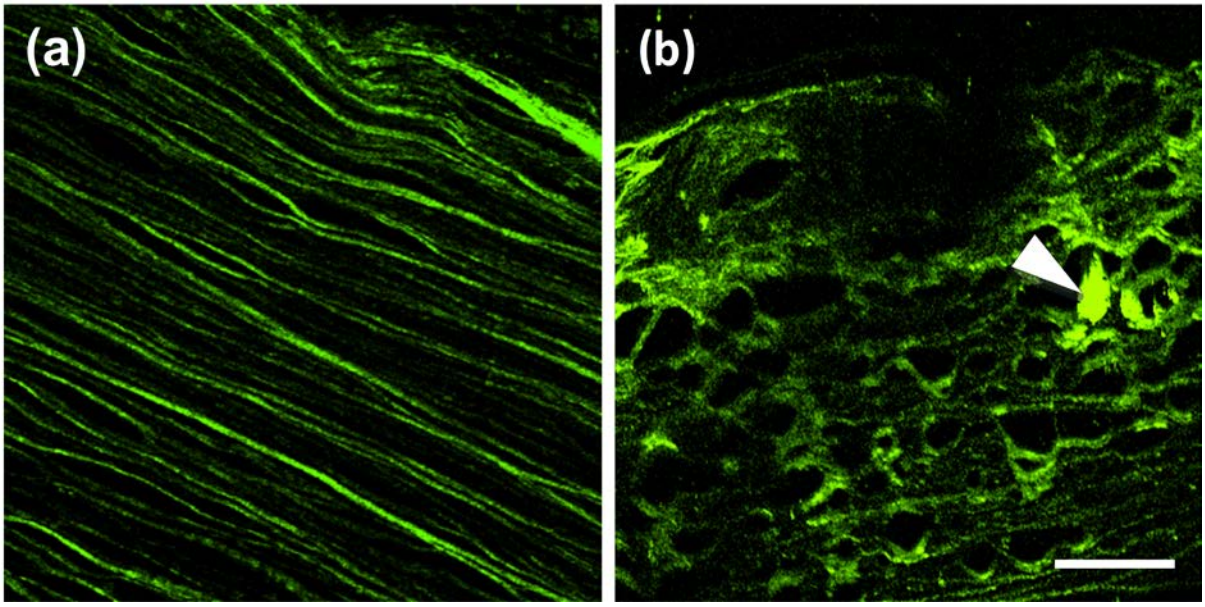

Figure 5. SHG images of human corneal biopsy samples. (a) Sample from a normal cornea (control); (b) Sample from a patient who has Lattice corneal dystrophy (LCD) disease. Collagen fibrils can be seen under SHG (green). Arrow indicates the formation of an amyloid. Scale bar: 20 μm.

Table 1. Powder SHG efficiencies of various amyloid-like peptides and human collagen subtypes.

Amyloid-like peptides / human collagens	$I^{2\omega}/I^{2\omega}$(sucrose)[a)]
IVK (IK_3)	3.31 ± 0.57
LIVAGD (LD_6)	3.06 ± 0.65
ILVAGS (IS_6)	1.96 ± 0.58
LIVAGK (LK_6)	0.95 ± 0.19
KLVFFAE (KE_7)	3.18 ± 0.67
GGVVIA (GA_6)	1.52 ± 0.43
DFNKF (DF_5)	0.89 ± 0.33
NFGAIL (NL_6)	0.76 ± 0.21
Collagen Type I	1.23 ± 0.36
Collagen Type II	0.41 ± 0.13
Collagen Type III	N.D. [b)]
Collagen Type IV	N.D. [b)]
Collagen Type V	N.D. [b)]

[a)] Value = Average ± standard deviation; [b)] N.D. = not detected.

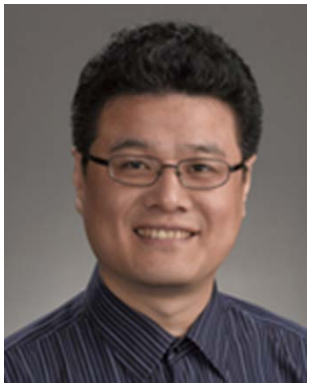

Dr. Ming Ni received his doctoral degree in Chemical Engineering from the University of Washington in 2004. Under the supervision of Dr. Buddy Ratner, his PhD project was to study the mechanism of osteoinduction by nacre (nacre also known as mother of pearl). After his graduation, he moved to Philadelphia and did two-year postdoc in Bioengineering at the University of Pennsylvania. Under the supervision of Dr. Paul Ducheyne, his project was to design, synthesize and characterize a novel sol-gel derived, nanostructured material that used for drug delivery applications. In 2007, he moved to Singapore, working as a research scientist at the Institute of Bioengineering and Nanotechnology (IBN), Agency for Science, Technology and Research (A*STAR). Currently, he is an assistant professor at Yachay Tech University, located at Urcuqui, Ecuador. His current research focuses on biomaterials. He is also interested in advanced scanning optical microscopy, microfluidics, stem cell therapy and drug delivery.

Shuangmu Zhuo received the Ph.D. degree in Optics Engineering from the Fujian Normal University, China, in 2012. He then joined the Singapore-MIT Alliance for Research and Technology as a Postdoctoral Research Fellow. He is currently a Professor in the College of Photonic and Electronic Engineering, Fujian Normal University, China. His research interests include the development and applications of nonlinear optical microscopy in biological and biomedical research.

Ciprian Iliescu received his BS degree and PhD degree from School of Mechanical Engineering, Polytechnic University of Bucharest in 1989 and 1999 respectively. While pursuing his PhD degree he worked at Baneasa S.A. where he was involved in the design and fabrication of pressure sensors. Between 2001 and 2003 he worked as postdoctoral fellow at NTU, and was involved in projects related to microphone, wafer level packaging of MEMS devices and RF microrelay. Between 2003 and 2017 he was with IBN, Singapore as research scientist and senior research scientist. He was also visiting PI @ IMT Bucharest where he set up the "Micro and Nanofluidic lab". Currently, he is senior research scientist with Bigheart @ NUS, Singapore. His current research projects relate to microfluidics for drug screening,

Peter So is a professor in the Department of Mechanical and Biological Engineering in the Massachusetts Institute of Technology. Prior to joining MIT, he obtained his Ph.D. from Princeton University in 1992 and subsequently worked as a postdoctoral associate in the Laboratory for Fluorescence Dynamics in the University of Illinois in Urban-Champaign. His research focuses on developing high resolution and high information content microscopic imaging instruments. Peter So is currently the Director of the MIT Laser Biomedical Research Center, a NIH NIBIB P41 research resource.

Prof. Jod S Mehta, Head of the Corneal Service Singapore National Eye Center (SNEC). Head of the Tissue Engineering and Stem Cell Group at the Singapore Eye Research Institute and Professor with DUKE-NUS GMS. Has trained 22 international fellows, 5 masters students and 6 PhD students. He leads a clinical service and runs a research program comprising of clinical and translational studies. His work is focused on corneal transplantation, femtosecond laser technology, corneal imaging, corneal infections, corneal refractive surgery, keratoprosthesis surgery and corneal genetics. He has published >340 peer-reviewed papers and 14 book chapters. Current H-index 47, citations 7440. He has given >100 invited plenary, symposium and named lectures globally. His research work as generated 15 patents, 4 of which have been licensed to companies.

Hanry Yu is a professor of physiology at the National University of Singapore and group leader at the Institute of Bioengineering and Nanotechnology, Agency for Science, Technology and Research. He was trained in cell biology at Duke University and Washington University in St Louis, USA, and European Molecular Biology Laboratories. His current research focuses on translating liver cell and tissue biology knowledge into industrial/medical applications through integration of cell sources, cell and tissue models of in vitro drug testing, and image-based analytics.

Charlotte A.E. Hauser is Professor of Bioscience at King Abdullah University of Science and Technology (KAUST), Thuwal, Saudi Arabia. Before joining KAUST, she was Principal Investigator at the Institute of Bioengineering and Nanotechnology, A*Star, Singapore, and Adjunct Professor at Nanyang Technological University, Singapore. After her Ph.D. in Molecular Biology at the Massachusetts Institute of Technology (MIT) and the University of Cologne, Germany, she joined INSERM in Paris, and the Max-Planck-Institute of Psychiatry in Munich, Germany. Furthermore, for almost ten years before returning to academia, she was founder and Managing Director of Octagene in Munich/Martinsried, Germany, where she developed the first truly human recombinant coagulation factor VIII (hFVIII) from a human cell line, approved in 2014 by FDA, EMEA and other regulatory authorities. This recombinant human clotting factor, available under the trade name of NUWIQ®, is the newest hFVIII replacement. Her honors and awards include awards from the German Federal Ministry of Science and Technology, France's Société des Amis des Sciences, and Bavarian Research Foundation. She holds over 20 U.S. patents of which the majority is owned or licensed to Nestle Skin Health, Octapharma AG, 3-D Matrix Co. Ltd., and PepNano. She is a Fellow of the American Institute for Medical and Biological Engineers (AIMBE). In 2015, she was elected as a member of the National Academy of Inventors in Washington. Her research includes molecular self-assembly, synthetic peptide biomaterials, amyloidogenesis, and regenerative therapies.

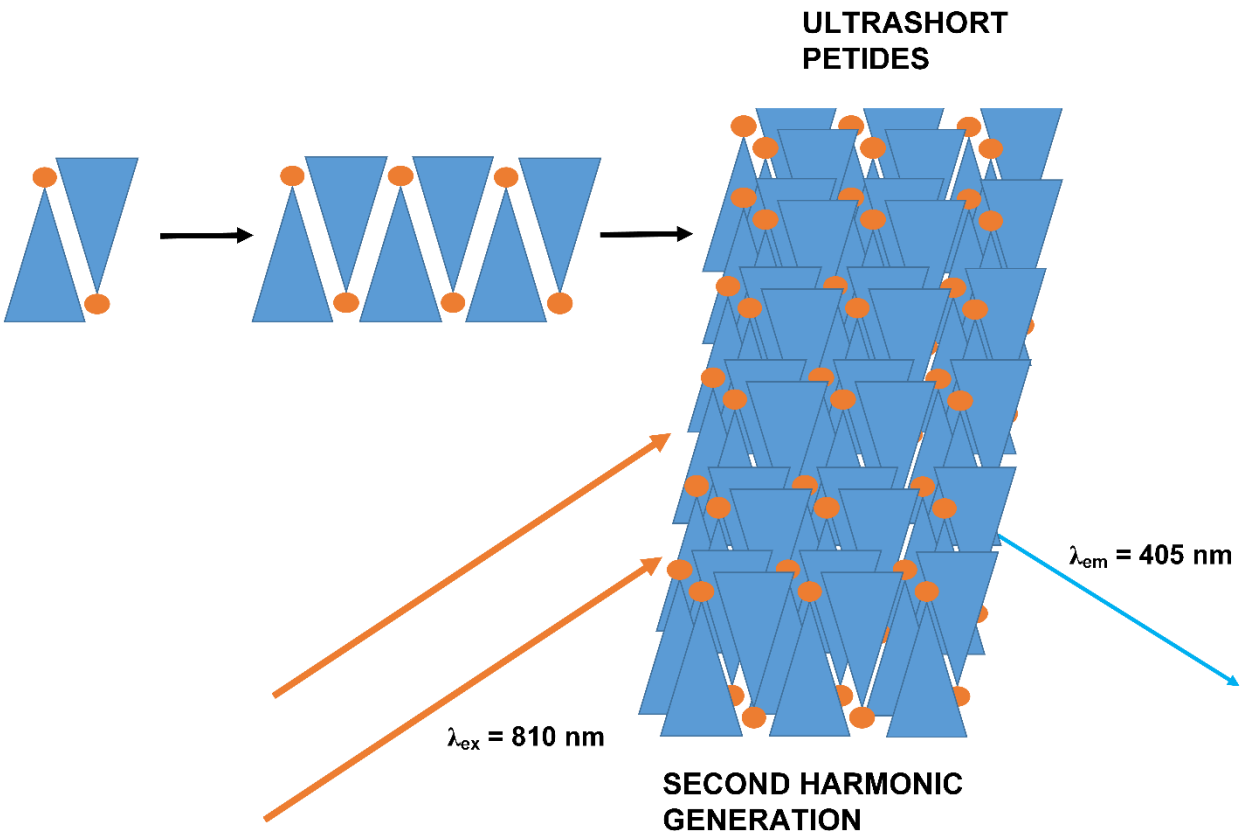

Ultrashort peptides undergo self-assembling and form nanofibers. In this schematic diagram, each blue triangle together with an orange circle represents an ultrashort peptide. The orange circle represents a hydrophilic headgroup and the blue triangle represents a hydrophobic tail with an increasing hydrophobicity. The ultrashort peptide nanofibers are able to generate second harmonic light. When excited at 810 nm, ultrashort peptide nanofibers emitted a sharp peak at 405 nm.

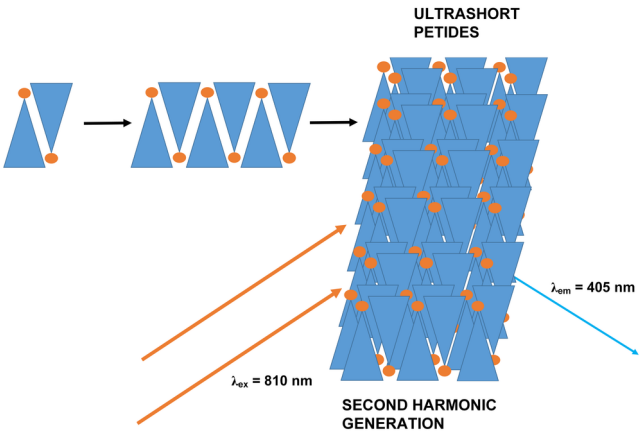

JBIO_201900065_Eye-catching color image.tif

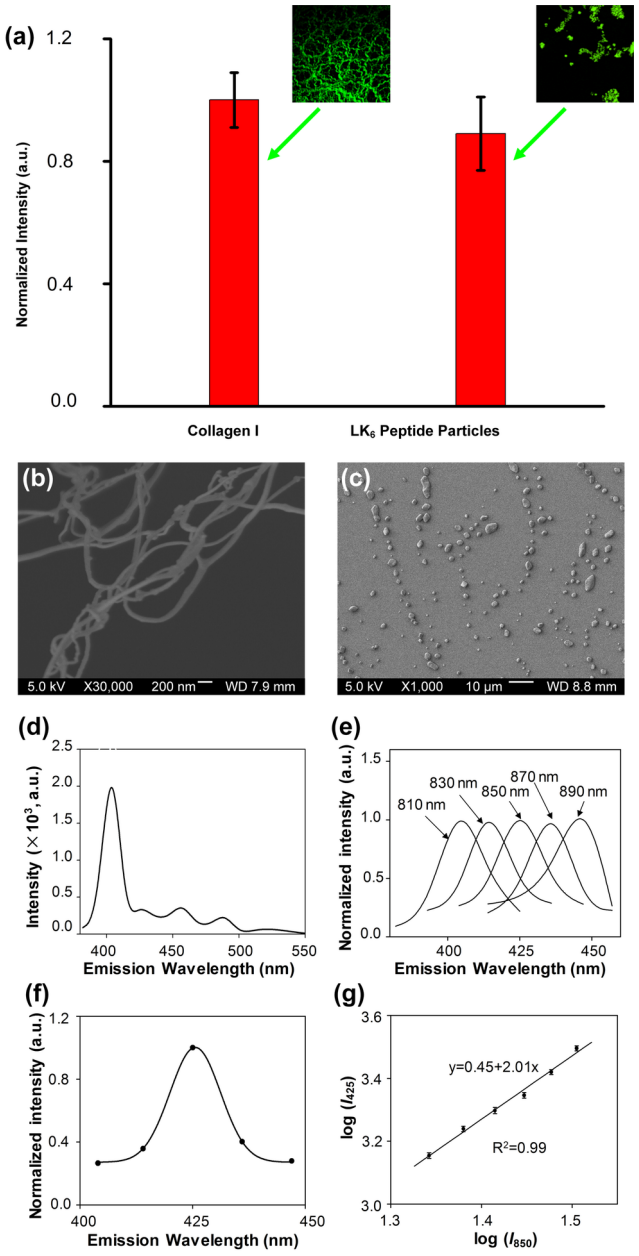

JBIO_201900065_Fig1.tif

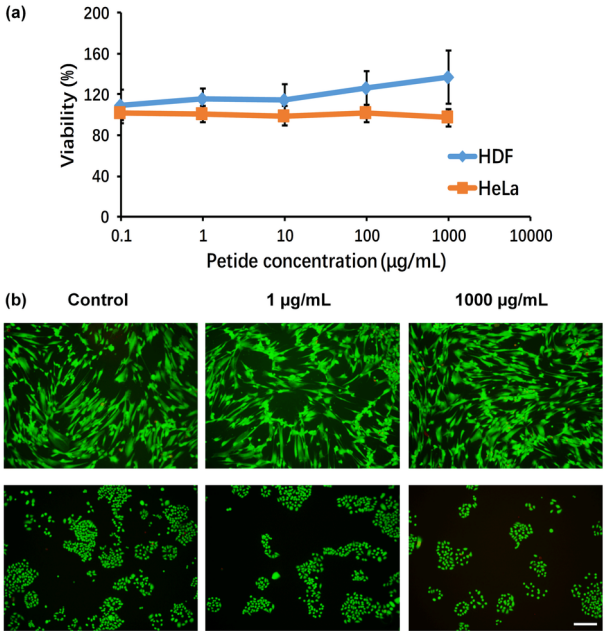

JBIO_201900065_Fig2.tif

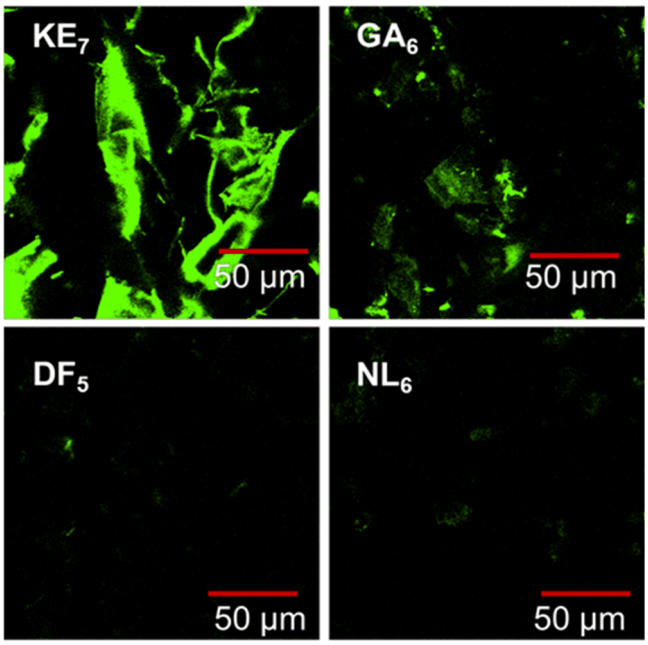

JBIO_201900065_Fig3.tif

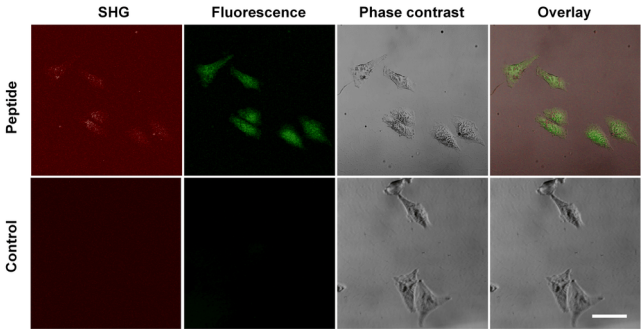

JBIO_201900065_Fig4.tif

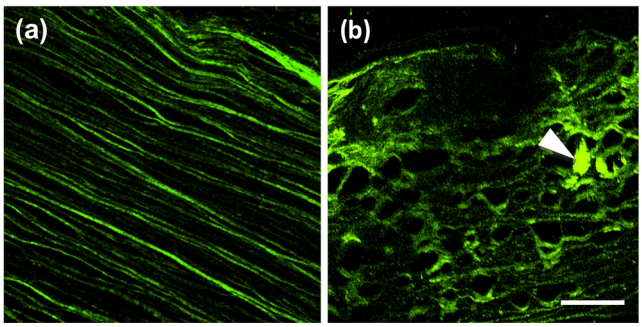

JBIO_201900065_Fig5.tif

Self-assembling amyloid-like peptides as exogenous second harmonic probes for bioimaging applications

Ming Ni [+]1,2, Shuangmu Zhuo [+]3, Ciprian Iliescu4,5, Peter T. C. So6,7, Jodhbir S. Mehta8, Hanry Yu1,6,9, Charlotte A. E. Hauser10

[1]Institute of Bioengineering and Nanotechnology, 31 Biopolis Way, The Nanos, Singapore 138669;
[2]School of Biological Sciences & Engineering, Yachay Tech University, Hacienda San José s/n, San Miguel de Urcuquí 100105, Ecuador
[3]Key Laboratory of Optoelectronic Science and Technology for Medicine of Ministry of Education, Fujian Normal University, Fuzhou, 350007, P. R. China
[4]BIGHEART, National University of Singapore, 14 Medical Drive, MD6, #14-01, 117597 Singapore
[5]Academy of Romanian Scientists, Splaiul Independentei nr. 54, Bucharest 050094, Romania
[6]Biosystems and Micromechanics IRG, Singapore-MIT Alliance for Research and Technology, 1 CREATE Way, #04-13/14 Enterprise Wing, 138602 Singapore;
[7]Department of Mechanical Engineering, Massachusetts Institute of Technology, 77 Massachusetts Avenue, Cambridge, MA 02139, USA
[8]Singapore Eye Institute and Singapore National Eye Center, 11 Third Hospital Avenue, 168751, Singapore
[9]Yong Loo Lin School of Medicine & Mechanobiology Institute, National University of Singapore, 14 Medical Drive, MD 9 #04-11, 117597, Singapore
[10]King Abdullah University of Science and Technology, Division of Biological & Environmental Science & Engineering, Laboratory for Nanomedicine, Al-Haytham Building (Bldg. 2), Office 4217, Thuwal 23955-6900, Kingdom of Saudi Arabia

[+] These authors contributed equally to this work.
* Corresponding Authors: M.N. (mingni.sg@gmail.com) or S.Z. (shuangmuzhuo@gmail.com) or H.Y. (hyu@ibn.a-star.edu.sg) or C.A.E.H. (charlotte.hauser@kaust.edu.sa).

ABSTRACT

Amyloid-like peptides are an ideal model for the mechanistic study of amyloidosis, which may lead to many human diseases, such as Alzheimer's. The paper reports a strong second harmonic generation (SHG) effect of amyloid-like peptides, having a signal equivalent to or even higher than those of endogenous collagen fibers. Several amyloid-like peptides (both synthetic and natural) were examined under SHG microscopy and shown they are SHG-active. These peptides can also be observed inside cells (*in vitro*). This interesting property can make these amyloid-like peptides second harmonic probes for bioimaging applications. Furthermore, SHG microscopy can provide a simple and label-free approach to detect amyloidosis. Lattice corneal dystrophy was chosen as a model disease of amyloidosis. Morphological difference between normal and diseased human corneal biopsy samples can be easily recognized, proving that SHG can be a useful tool for disease diagnosis.

Keywords: bioimaging, non-linear optical materials, second harmonic generation, self-assembly, ultrashort peptides.

1. Introduction

Amyloid-like peptides are responsible for amyloidosis which is an important feature for several human diseases, including Alzheimer (AD) [1-2], Parkinson [3], type II diabetes [4], cataracts [5], or lattice corneal dystrophy (LCD) [6]. The inhibition of amyloid-like peptides production is a promising strategy for the development of therapeutic agents to treat such diseases. However, the mechanism of amyloidosis is still unclear. One logical mechanistic approach is to study how these amyloid-like peptides/proteins fold or misfold [2, 7]. In this direction, ultrashort peptides (having only three to seven amino acids) provide us an ideal model for mechanistic studies. For example, GGVVIA (GA_6) and KLVFFAE (KE_7), can self-assemble into amyloid-like aggregates [8-9]. The previously mentioned peptides are also known as the core sequence of amyloid-β (A_β). A_β is the major component in the amyloid aggregates responsible for AD. Besides ultrashort peptides that can be found in natural peptides/proteins, several designed synthetic ultrashort peptides, such as IVD (ID_3) and LIVAGD (LD_6), have shown similar behavior [9-10]. Both the natural and synthetic peptides are amyloid-like peptides. Ultrashort amyloid-like peptides can not only be useful for screening of amyloid inhibitors [10-11], but also as a new type of biomaterials with desirable properties such as biocompatibility and biological activities [8-9, 12-13]. They all form cross-β peptide structure at a molecular level. Mechanically they are rigid, with strength comparable to steel [14]. Morphologically they are helical fibers of micrometers in length but only 7-10 nm in diameter [15], having a similar morphology to collagen fibers [10, 16]. Supramolecular assemblies of collagen in tissues have been visualized by SHG microscopy [17]. In particular, collagen I and collagen II have been proven to efficiently produce SHG signals [17-18]. SHG has been applied to investigate rat and human corneal samples [19-22]. Collagen fibrils in cornea were observed under SHG microscopy without any labelling. The orientation,

morphology and submicron heterogeneity of collagen fibers were quantitatively analyzed by SHG, which potentially can be used for in vivo diagnosis of corneal diseases, such as LCD. Besides collagen is used as a biomarker for LCD, extracellular deposition of amyloid β within cornea is commonly thought as the main reason for LCD. Inspired by these findings, we demonstrate here the non-linear optical (NLO) properties of self-assembled ultrashort amyloid-like peptides [23] and explore their potentials as novel organic probes for SHG imaging. Besides significant advantages over the conventional fluorescence imaging techniques such as deeper optical penetration, lower photo-damage and longer observation time [24-27], SHG microscopy provides a simple and label-free approach to detect amyloid-like peptides, which can be a useful tool for disease diagnosis, especially for LCD.

2. Materials and Methods

2.1 Ultrashort Amyloid-Like Peptides

Amyloid-like peptides were purchased from the American Peptide Company (purity ≥95%). The peptide sequences were confirmed by liquid chromatography-mass spectrometry (LC-MS). Net peptide content varied between 70% and 85%. All peptides were acetylated at the N terminus. Peptide handling and hydrogel preparation were done as reported previously [10, 28].

2.2 Peptide Particles

The preparation of the peptide particles was performed by hydrodynamic focusing, method described in previous work [29-31]. The particle size was determined by scanning electron microscopy, showing a grain size of around 5 μm.

2.3 Cell Culture

Both HeLa and human dermal fibroblasts were cultured in DMEM supplemented with 10% fetal bovine serum and 1% penicillin/streptomycin (Life Technologies, Singapore).

2.4 Human corneal biopsy samples

The human corneal biopsy samples were provided by Singapore General Hospital. The normal tissue was from a seventy-eight year-old Caucasian male. The diseased tissue was from a sixty-year-old female who has lattice corneal dystrophy (LCD). The study was approved by the institutional review board (IRB) from Singhealth.

2.5 SHG Imaging

SHG images were acquired using a commercial laser scanning microscopic imaging system (Zeiss LSM 510 META, Jena, Germany) coupled to a mode-locked femtosecond Ti: sapphire laser (Mai-Tai broadband, Spectra-Physics), tunable from 710 nm to 990 nm. To achieve spectral analysis and detect the SHG signal, we used the META detector with 32-gated photon counting module [17].

3 Results and Discussions

3.1 A hexamer peptide is collagen-like and SHG-active

To test whether these amyloid-like peptides are SHG-active, we first investigated a hexamer peptide, Ac-LIVAGK-NH_2, (LK_6). Peptide powder was dissolved in pure water and peptide microparticles were assembled on a microfluidic chip using hydrodynamic focusing techniques. The resulting peptide microparicles were examined under SHG microscopy. During the whole experiments, only the backscattered geometry was employed because it is the only suitable configuration for *in vivo* imaging [26]. We chose collagen I as a control, being shown that SHG microscopy can visualize supramolecular assembly of collagen in tissues [26]. Both collagen I and peptide particles showed SHG signals with comparable intensity. This is shown in **Figure 1a** where the SHG signal from the collagen fibers of a rat liver tissue was compared with

the signal from LK_6 peptide particles (instrument settings for both SHG imaging being the same). The fine structures of collagen and peptide particles can be clearly seen under SHG and SEM- **Figure 1b and c**. Moreover, LK_6 peptide exhibits typical SHG characteristics. Excited at 810 nm, LK_6 emitted a sharp SHG peak at 405 nm (**Figure 1d**). This is a main characteristic of SHG: two photons can be converted into one photon at exactly half of the wavelength. We then examined the excitation wavelength tunability of SHG signals from LK_6 peptide. In **Figure 1e**, as the excitation wavelength was increased from 810 to 890 nm, the wavelength of the SHG signals from the LK_6 peptide particles increased from 405 to 445 nm respectively. The opportunity of tuning the excitation wavelength gives the advantage of best matching with the optical properties of the sample. It is known that a biological sample (cells/tissues) presents auto-fluorescence. It should be noted that the SHG emission is significantly enhanced when exciting with a quasi-resonant scheme (~720 nm maximum). However, longer wavelengths will result in greater depth of penetration because of reduced scattering and also avoid auto-fluorescent absorption bands in tissues. In this work, we used excitation wavelength ranging from 810 to 890 nm, which falls in the so called ¨therapeutic window¨ or ¨optical window¨. The common problems encounter by conventional fluorescent microscopy are circumvented. In addition, a further increase of the penetration depth in tissues can be achieved by simply increasing excitation wavelength. **Figure 1f** showed the emission wavelength data of the SHG signal (λ_{ex} = 850 nm). The data in the graph was fitted to a Gaussian curve exhibiting a maximum at 425nm, which is exactly half the excitation wavelength of 850 nm. The bandwidth (full width at half-maximum of Gaussian distribution, FWHM) was narrow (~10 nm) and it obeyed a $1/\sqrt{2}$ relationship to the corresponding wavelength profile of the fundamental beam (~15 nm). Moreover, the dependence of the output signal on irradiation intensity

was measured by varying the 850nm excitation intensity. The linear regression, applied to the log-log plots (**Equation 1**), revealed a quadratic power dependence of SHG intensity to power intensity, as shown in the **Figure 1g**.

$$\log[I_{425}] = 0.45 + 2.01 \times \log[I_{850}] \quad (1)$$

The intensity of SHG signal is proportional to the square of the incident laser intensity. This confirmed the two-photon nature of the emission from LK_6 peptide.

3.2 Cytocompatibility of a hexamer peptide

In order to use LK_6 for bioimaging applications, such as *in vitro* cells monitoring or *in vivo* imaging, we assessed the cytotoxicity of LK_6 using MTS test and live/dead assay with two human cell lines, human epithelial carcinoma cells (HeLa) and primary human dermal fibroblasts (HDF) (**Figure 2**). Cells were exposed to cell culture media containing different concentrations of LK_6 solution (0.1 to 1000 µg/mL) and incubated for 48 h. Cell viability at various LK_6 concentrations was either equivalent to or even higher than that of untreated cells over the whole concentration range which was tested in this study (**Figure 2a)**. To further confirm these results, we stained cells with or without peptide exposure using solutions containing a mixture of calcein AM and ethidium homodimer-1 (EthD-1). Calcein AM can penetrate cell membrane and be converted within the cell to membrane impermeable green fluorescent calcein, while red fluorescent EthD-1 is unable to permeate the intact cell membrane of living cells. **Figure 2 b** shows the representative live/dead images of cells in response to LK_6 solutions (1 and 1000 µg/mL). LK_6 displayed no toxicity to both HDF and HeLa cells, in agreement with the results of the MTS assays.

3.3 Comparison of synthetic and natural amyloid-like peptides under SHG microscopy

Several other amyloid-like peptides, including both natural amyloidogenic core sequences (NL_6, DF_5, GA_6, and KE_7) and designed synthetic peptides (LD_6, IS_6 and IK_3) were examined under SHG excitation. The peptide sequences are listed in Table 1. All these peptides are SHG-active. We used a powder technique developed by Kurtz and Perry [32] to evaluate the SHG efficiency of these second-order nonlinear optical materials. Sucrose was chosen as control to evaluate SHG efficiencies [33]. In Table 1, all tested amyloid-like peptides showed higher or equivalent SHG efficiency compared to sucrose. These can be explained through their molecular structures. LD_6 is known to form hydrogel at much lower concentrations compared to LK_6. The trimer IK_3 has larger dipole moment compared to LK_6. Human collagen subtypes I to V were also examined (**Table 1**) for their SHG activity. Only Collagen type I and II showed positive results, aspect that is in concordance with the previous findings reported in the literature [18, 34]. Moreover, some amyloid-like peptides such as IVK, LIVAGD or even ILVAGS showed even higher SHG efficiency than collagen subtypes (I and II). This suggests the opportunity of using these materials as SHG probes.

The investigation of the SHG efficiency for four natural amyloidogenic core sequences indicates the following order: $KE_7 > GA_6 > DF_5 > NL_6$ (**Table 1 and Figure 3**). KE_7 (KLVFFAE), containing its diphenylalanine (FF) motif, showed the highest SHG efficiency among these four peptides. However, its SHG efficiency is similar as that of IK_3. It is noteworthy that IK_3 is an aliphatic peptide. Aromatic residues such as tyrosine and tryptophan are known to be used as an endogenous molecular probe of peptides and proteins for SHG at the air-water interface [35]. However, our results indicated that aromatic residues are not necessary for higher SHG efficiency. LD_6, IS_6, LK_6 and IK_3 are all aliphatic and lacking aromatic residues, clearly makes them a unique type of peptides for SHG applications. These peptides are amphiphilic [10, 16], consisting of

an aliphatic amino acid tail of decreasing hydrophobicity and a hydrophilic head. They can self-assembly via parallel-antiparallel α-helical pairs and subsequent stacking into β-turn fibrils, which show striking similarity to collagen fibers [16]. We reasoned that the origin of these amyloid-like peptides' SHG activity comes from their nanostructures. A recent study showed that the origin of SHG signals from collagen fibers possibly lies in their peptide bonds [36]. The collagen fiber building blocks were mimicked by tri-amino acid peptides PPG and GGG (P and G are the one letter code for Proline and Glycine respectively).

3.4 A hexamer peptide as a second harmonic probe for in vitro cell imaging

Another possible application for LK_6 is to use it for high-resolution cell imaging. To this end, HeLa cells were incubated with biotin-conjugated LK_6 for 4 h and then fixed for immune staining. LK_6 peptides were visualized by both SHG and confocal fluorescence microscopy. In **Figure 4**, biotin-conjugated peptides displayed green color when DyLight™ 488-conjugated NeutrAvidin™ (Thermo Scientific, Singapore, Prod #: 22832) was added. Meanwhile, amyloid-like peptides displayed pseudo red color under SHG. These results revealed two interesting features of the investigated amyloid-like peptides: 1) they can be visualized under SHG without any label; 2) they can be up-taken by cells. We want to point out that when attaching additional labels such as chromophores to the amyloid-like peptide structure for bioimaging purposes, it may easily change the molecular properties of the native peptide molecules. Thus, additional changes of the peptide molecule are time consuming and asking for more costly synthetic approaches. Hence, using amyloid-like peptides in their native structure for a label-free SHG bioimaging technology could certainly be useful as an attractive and minimal-invasive diagnostic tool.

In addition, a molecular-level property of the nonlinearity, i.e., the first hyperpolarizability, β, was measured by Hyper Rayleigh Scattering (HRS). The first hyperpolarizability of these trimers was about 0.087×10^{-30} esu [36]. However, the first hyperpolarizability of collagen I was found to be $(1250 \pm 20) \times 10^{-30}$ esu [36], which could be viewed as ten thousand trimers combining together. In terms of SHG signals, collagen consists a triple helix structure, which shows very strong SHG signals. Single collagen amino acid such as glycine, proline and hydroproline does not show SHG signals as strong as collagen fibrils. We hypothesize that the aggregation of these tripeptides gives the much stronger SHG signals in comparison with isolated tripeptides. Based on the non-linearity of the intrinsic peptide bonds and their aggregation capability, these amyloid-like peptides can generate SHG signals, just like collagen.

3.5 Diseased and normal human corneal biopsy samples examined by SHG microscopy

More interestingly, when we examined the human corneal biopsy samples (**Figure 5a and 5b**), both amyloids (indicated by arrow) and collagen can be seen. The human corneal biopsy samples were provided by Singapore General Hospital. The normal tissue was from a seventy-eight year-old Caucasian male. The diseased tissue was from a sixty-year-old female who has lattice corneal dystrophy (LCD). Under SHG, the normal corneal sample showed collagen fibrils aligned as parallel straight lines in stroma. By contrast diseased samples showed collagen fibrils became curved and thicker. The thickened collagen fibrils could be due to amyloid deposits [37]. Thus, SHG provides us a new diagnostic tool for lattice corneal dystrophy (LCD) that is superior to the existing histological staining methods: SHG being a label-free method.

4. Conclusions

We demonstrated that amyloid-like peptides are nonlinear optical materials showing strong SHG signals and a quadratical dependence of SHG intensity to power intensity. Amyloid-like peptides show no cytotoxic effect to human cells and can be observed inside cells without fluorescent labelling, which make them suitable as second harmonic probes. Amyloid-like peptide nanomaterials hold great potential in nanotechnology and nanomedicine. We assembled amyloid peptide microparticles via hydrodynamic focusing on a microfluidic chip. We could encapsulate small molecule drugs, DNA or RNA when we assembled them on chip. Their nonlinear optical properties hold promise for new bioimaging applications. The development of SHG microendoscopy [38] could open more opportunities for using amyloid-like peptides as a SHG probe for more bioimaging applications. The imaging capability in combination with therapeutic capability via drug encapsulation will make these amyloid-like peptides interesting theranostic agents.

Acknowledgements

This work was funded by the Institute of Bioengineering and Nanotechnology (Biomedical Research Council, Agency for Science, Technology and Research, Singapore). S.Z. thanks the SMART Scholars Programme, the National Natural Science Foundation of China (81771881), the Natural Science Foundation of Fujian Province (2018J07004), the Special Funds of the Central Government Guiding Local Science and Technology Development (2017L3009) for financial support.

Author Information: The authors declare no competing financial interests.

References

[1] Soto C, Brañes MC, Alvarez J, Inestrosa NC. Structural Determinants of the Alzheimer's Amyloid β-Peptide. J. Neurochem. 1994; 63: 1191-8.

[2] Chiti F, Dobson CM. Protein Misfolding, Functional Amyloid, And Human Disease. Annu. Rev. Biochem. 2006; 75: 333-66.

[3] Polymeropoulos MH, Lavedan C, Leroy E, Ide SE, Dehejia A, Dutra A, Pike B, Root H, Rubenstein J, Boyer R. Mutation In The A-Synuclein Gene Identified In Families With Parkinson's Disease. Science 1997; 276: 2045-7.

[4] Clark A, Lewis C, Willis A, Cooper G, Morris J, Reid K, Turner R. Islet Amyloid Formed From Diabetes-Associated Peptide May Be Pathogenic In Type-2 Diabetes. Lancet 1987; 330: 231-4.

[5] Goldstein LE, Muffat JA, Cherny RA, Moir RD, Ericsson MH, Huang X, Mavros C, Coccia JA, Faget KY, Fitch KA. Cytosolic B-Amyloid Deposition And Supranuclear Cataracts In Lenses From People With Alzheimer's Disease. Lancet 2003; 361: 1258-65.

[6] Gorevic PD, Munoz PC, Gorgone G, Purcell JJ, Rodrigues M, Ghiso J, Levy E, Haltia M, Frangione B. Amyloidosis Due To A Mutation Of The Gelsolin Gene In An American Family With Lattice Corneal Dystrophy Type II. N. Eng. J. Medicine 1991; 325: 1780-5.

[7] Dobson CM. Protein Folding And Misfolding. Nature 2003; 426: 884-90.

[8] Kirschner DA, Inouye H, Duffy LK, Sinclair A, Lind M, Selkoe DJ. Synthetic Peptide Homologous To Beta Protein From Alzheimer Disease Forms Amyloid-Like Fibrils In Vitro. P. Natl. Acad. Sci. USA 1987; 84: 6953-7.

[9] Hauser CA, Maurer-Stroh S, Martins IC. Amyloid-Based Nanosensors And Nanodevices. Chem. Soc. Rev. 2014; 43: 5326-45.

[10] Hauser CA, Deng R, Mishra A, Loo Y, Khoe U, Zhuang F, Cheong DW, Accardo A, Sullivan MB, Riekel C. Natural Tri-To Hexapeptides Self-Assemble In Water To Amyloid B-Type Fiber Aggregates By Unexpected A-Helical Intermediate Structures. P. Natl. Acad. Sci. USA 2011; 108: 1361-6.

[11] Azriel R, Gazit E. Analysis Of The Minimal Amyloid-Forming Fragment Of The Islet Amyloid Polypeptide An Experimental Support For The Key Role Of The Phenylalanine Residue In Amyloid Formation. J. Biol. Chem. 2001; 276: 34156-61.

[12] Ni M, Zhuo S. Applications of self-assembling ultrashort peptides in bionanotechnology. RSC Adv. 2019; 9: 844-52.

[13] Cherny I, Gazit E. Amyloids: not only pathological agents but also ordered nanomaterials. Angew. Chem. Int. Edit. 2008; 47: 4062-9.

[14] Smith JF, Knowles TP, Dobson CM, MacPhee CE, Welland ME. Characterization Of The Nanoscale Properties Of Individual Amyloid Fibrils. P. Natl. Acad. Sci. USA 2006; 103:15806-11.

[15] Shirahama T, Cohen AS. High-Resolution Electron Microscopic Analysis Of The Amyloid Fibril. J. Cell. Biol. 1967; 33: 679-708.

[16] Mishra A, Loo Y, Deng R, Chuah YJ, Hee HT, Ying JY, Hauser CA. Ultrasmall Natural Peptides Self-Assemble To Strong Temperature-Resistant Helical Fibers In Scaffolds Suitable For Tissue Engineering. Nano Today 2011; 6: 232-9.

[17] Zhuo S, Chen J, Wu G, Xie S, Zheng L, Jiang X, Zhu X. Quantitatively Linking Collagen Alteration And Epithelial Tumor Progression By Second Harmonic Generation Microscopy. Appl. Phys. Lett. 2010; 96: 213704.

[18] Chen X, Nadiarynkh O, Plotnikov S, Campagnola PJ. Second Harmonic Generation Microscopy For Quantitative Analysis Of Collagen Fibrillar Structure. Nat. Protoc. 2012; 7: 654-69.

[19] Latour G, Gusachenko I, Kowalczuk L, Lamarre I, Schanne-Klein MC. In vivo structural imaging of the cornea by polarization-resolved second harmonic microscopy. Biomed. Opt. Express 2012; 3: 1-15.
[20] Bancelin S, Aime C, Gusachenko I, Kowalczuk L, Latour G, Coradin G, Schanne-Klein MC, Determination of collagen fibril size via absolute measurements of second-harmonic generation signals. Nat. Commun. 2014; 5: 4920.
[21] Mercatelli R, Ratto F, Rossi F, Tatini F, Menabuoni L, Malandrini A, Nicoletti R, Pini R, Pavone FS, Cicchi RR. Three-dimensional mapping of the orientation of collagen corneal lamellae in healthy and keratoconic human corneas using SHG microscopy. J. Biophoton. 2017; 10: 75-83.
[22] Mercatelli R, Mattana S, Capozzol Li, Ratto F, Rossi F, Pini R, Fioretto D, Pavone FS, Caponi S, Cicchi R. Morpho-mechanics of human collagen superstructures revealed by all-optical correlative micro-spectroscopies. Communications Biology 2019; 2: 117.
[23] Franken PA, Hill AE, Peters CE, Weinreich G. Generation Of Optical Harmonics. Phys. Rev. Lett., 1961; 7: 118-9.
[24] Zipfel WR, Williams RM, Christie R, Nikitin AY, Hyman BT, Webb WW. Live Tissue Intrinsic Emission Microscopy Using Multiphoton-Excited Native Fluorescence And Second Harmonic Generation. P. Natl. Acad. Sci. USA 2003; 100: 7075-80.
[25] Pantazis P, Maloney J, Wu D, Fraser SE. Second Harmonic Generating (SHG) Nanoprobes For In Vivo Imaging. P. Natl. Acad. Sci. USA 2010; 107: 14535-40.
[26] Campagnola PJ, Loew LM. Second-harmonic imaging microscopy for visualizing biomolecular arrays in cells, tissues and organisms. Nat. Biotech. 2003; 21: 1356-60.
[27] Yu F, Zhuo S, Qu Y, Choudhury D, Wang Z, Iliescu C, Yu H. On Chip Two-Photon Metabolic Imaging For Drug Toxicity Testing. Biomicrofluidics 2017; 11: 034108.
[28] Chan KH, Lee WH, Ni M, Loo Y, Hauser CAE. C-Terminal Residue of Ultrashort Peptides Impacts on Molecular Self-Assembly, Hydrogelation, and Interaction with Small-Molecule Drugs. Sci. Rep. 2018; 8: 17127.
[29] Ni M, Tresset G, Iliescu C. Self-Assembled Polysulfone Nanoparticles Using Microfluidic Chip. Sensor. Actuat. B-Chem. 2017; 252: 458-62.
[30] Iliescu C, Tresset G. Microfluidics-Driven Strategy for Size-Controlled DNA Compaction by Slow Diffusion through Water Stream. Chem. Mater. 2015; 27: 8193-7.
[31] Tresset G, Marculescu C, Salonen A, Ni M, Iliescu C. Fine Control Over The Size Of Surfactant–Polyelectrolyte Nanoparticles By Hydrodynamic Flow Focusing. Anal. Chem., 2013; 85: 5850-6.
[32] Kurtz S, Perry T. A Powder Technique For The Evaluation Of Nonlinear Optical Materials. J. Appl. Phys., 1968; 39: 3798-813.
[33] Bourhill G, Mansour K, Perry KJ, Khundkar L, Sleva ET, Kern R, Perry JW, Williams ID, Kurtz SK. Powder Second Harmonic Generation Efficiencies Of Saccharide Materials. Chem. Mater. 1993; 5: 802-8.
[34] Su PJ, Chen WL, Li TH, Chou CK, Chen TH, Ho YY, Huang CH, Chang SJ, Huang YY, Lee HS. The Discrimination Of Type I And Type II Collagen And The Label-Free Imaging Of Engineered Cartilage Tissue. Biomaterials 2010; 31: 9415-21.
[35] Nasir MN, Benichou E, Loison C, Russier-Antoine I, Besson F, Brevet PF. Influence Of The Tyrosine Environment On The Second Harmonic Generation Of Iturinic Antimicrobial Lipopeptides At The Air–Water Interface. Phys. Chem. Chem. Phys., 2013; 15: 19919-24.
[36] Duboisset J, Deniset-Besseau A, Benichou E, Russier-Antoine I, Lascoux N, Jonin C, Hache F, Schanne-Klein MC, Brevet PF. A Bottom-Up Approach To Build The Hyperpolarizability Of Peptides And Proteins From Their Amino Acids. J. Phys. Chem. B 2013; 117: 9877-81.

[37] Anandalakshmi V, Murugan E, Leng EGT, Ting LW, Chaurasia SS, Yamazaki T, Nagashima T, George BL, Peh GSL, Pervushin K, Lakshminarayanan R, Mehta JS. Effect of position-specific single-point mutations and biophysical characterization of amyloidogenic peptide fragments identified from lattice corneal dystrophy patients. Biochem J. 2017; 474:1705-25.
[38] Zhang Y, Akins ML, Murari K, Xi J, Li MJ, Luby-Phelps K, Mahendroo M, Li X. A Compact Fiber-Optic SHG Scanning Endomicroscope And Its Application To Visualize Cervical Remodeling During Pregnancy. P. Natl. Acad. Sci. USA 2012; 109: 12878-83.

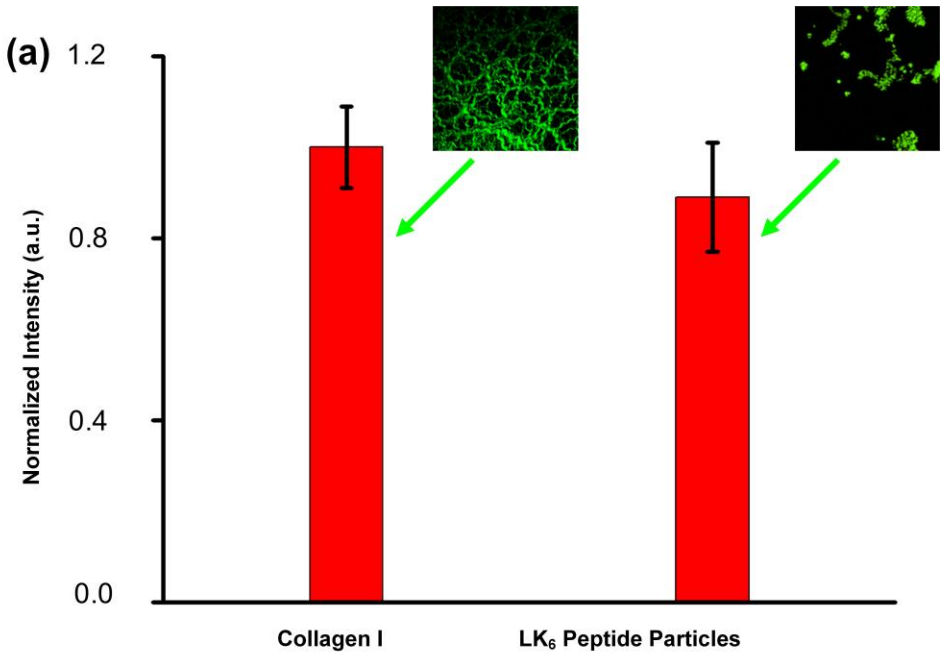

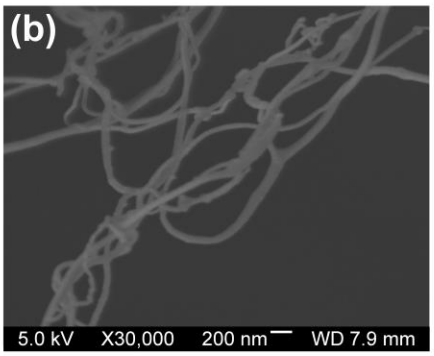

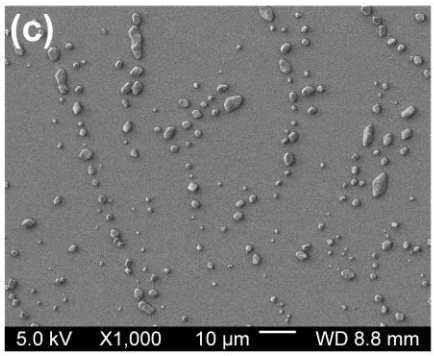

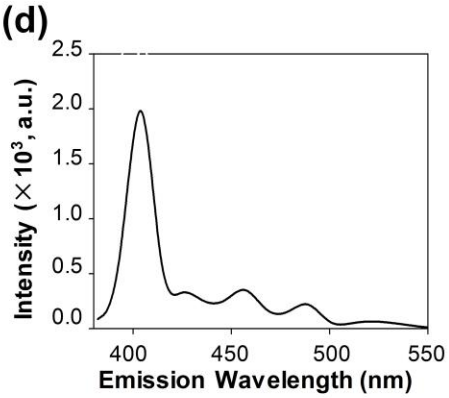

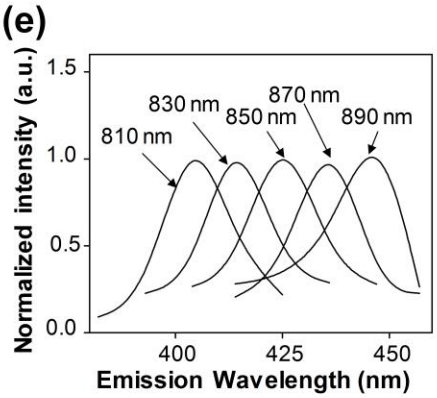

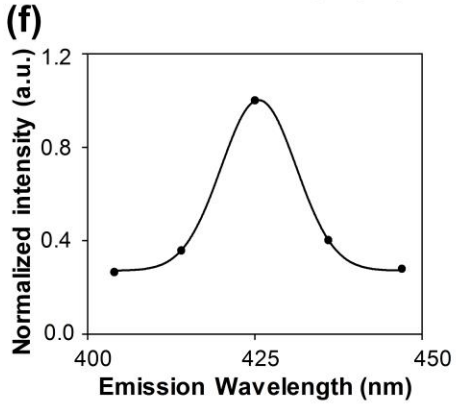

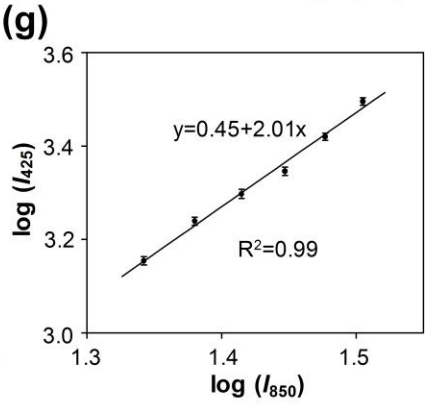

Figure 1. (a) Comparison of the SHG signal intensity from endogenous collagen I to LK6 peptide particles. Five spots from each image were chosen and the SHG signal intensity was normalized to collagen I (mean ± standard deviation, n=5); (b) SEM image of collagen fibers; (c) SEM image peptide particles. d) SHG signal spectrum of LK_6 peptide. Signal was ranging from 380 to 550 nm with excitation wavelength of 810 nm and peak emission wavelength was shown at 405 nm; (e) Spectral peaks at various excitation wavelengths spanning a broad spectral region (810-890 nm); (f) Emission λ-scan of the SHG signal (λ_{ex} = 850 nm) acquired from SHG imaging of LK_6 peptide particles. The solid spheres represent back scattering SHG data and the solid line represents a Gaussian fit. The full width at half-maximum of the fitted curve bears a $1/\sqrt{2}$ relation to the spectral profile of the corresponding beam; (g) Log-log plot of the above SHG signal measurements demonstrating a $\log[I425] = 0.45 + 2.01 \times \log[I850]$ dependence, quadratic to a good approximation, consistent with nonlinear second order optical upconversion.

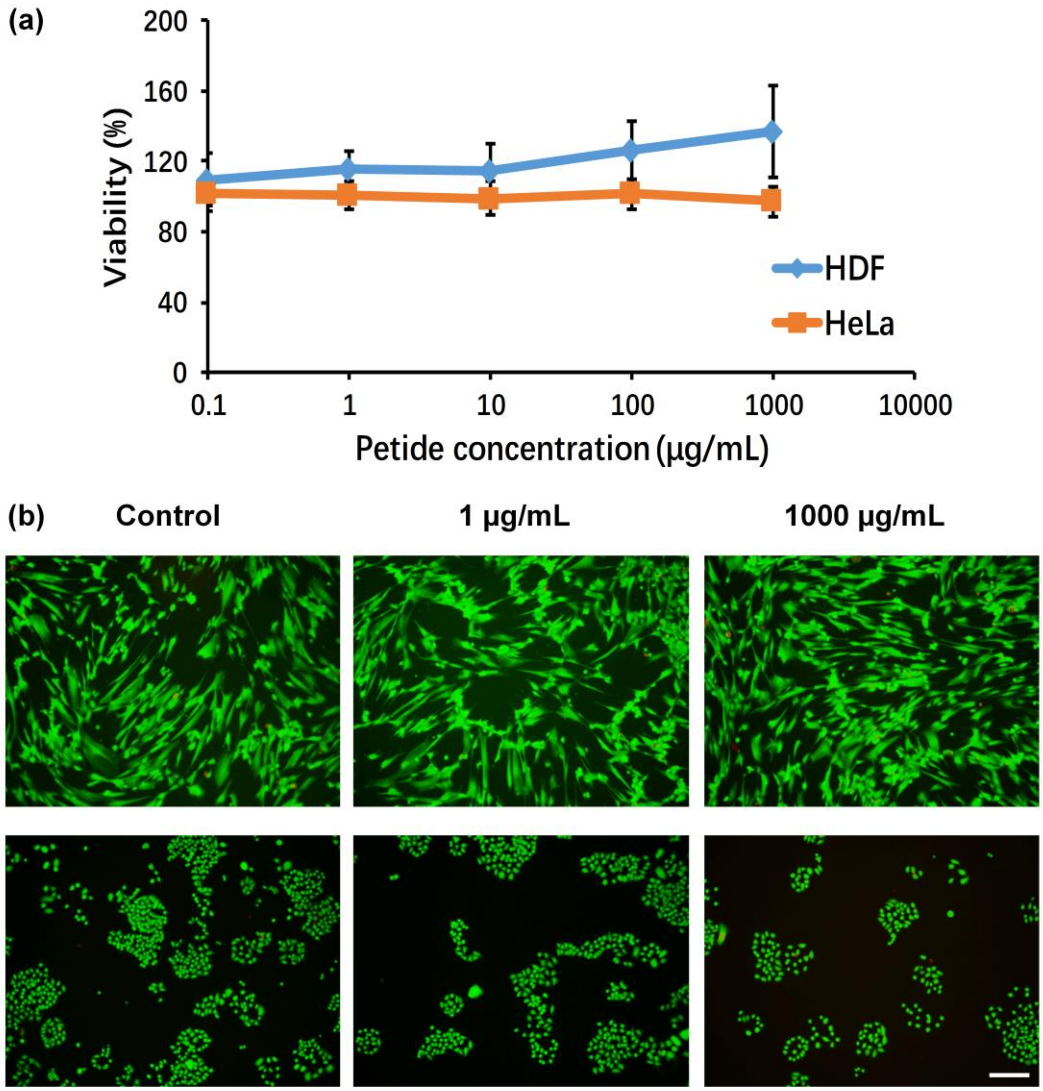

Figure 2. Cytotoxicity studies of LK6 peptide treated HDF and HeLa cells. (a) Cell viability at 48 h of HDF and HeLa cells incubated with cell culture media containing LK_6 peptide solutions, as determined using MTS assay (mean ± standard deviation, n=9). Concentrations ranged from 0.1 to 1000 μg/mL. (b) Cytotoxicity determined by Calcein AM/EthD-1 (live/dead, green/red) staining method after 48 h treated with 1 and 1000 μg/mL LK_6 peptide solutions using non-treated cells as control. Scale bar: 100 μm.

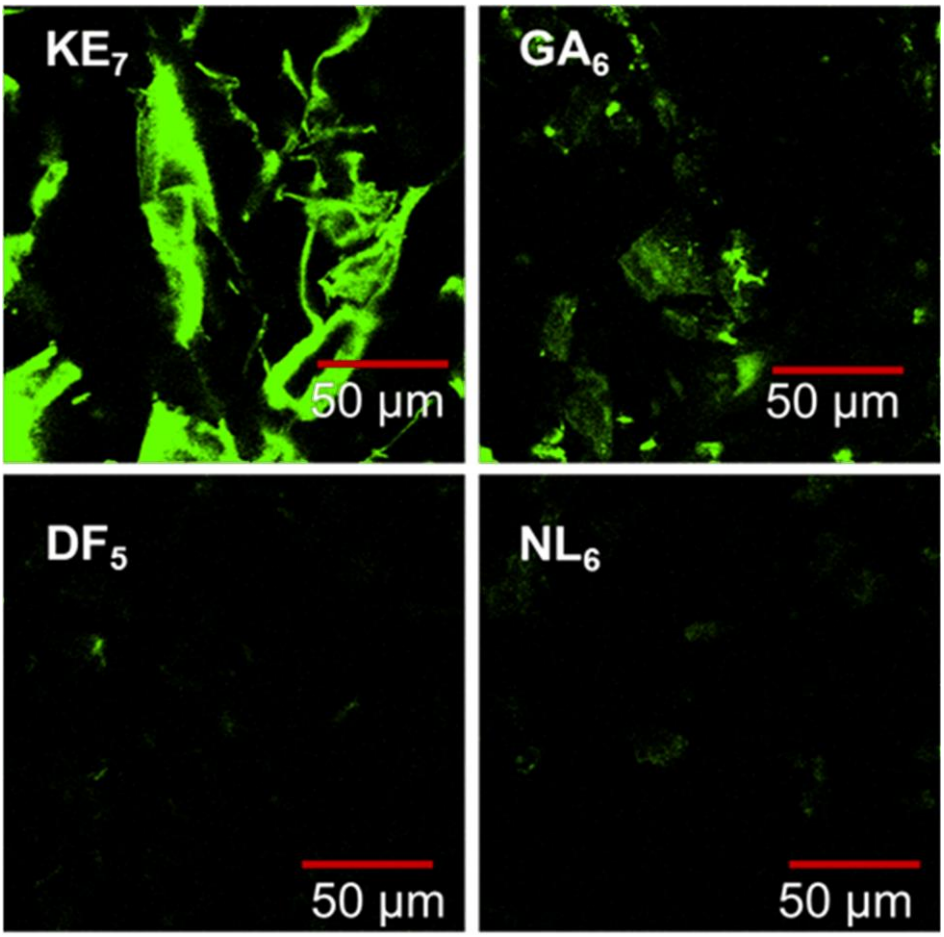

Figure 3. SHG images of four pristine peptides with natural amyloidogenic core sequences. The whole window was covered with pristine peptides. However, only part of the peptides can be visualized under SHG microscopy. The SHG intensity follows the order of KE7 > GA6 > DF5 > NL6. Scale bars: 50 μm.

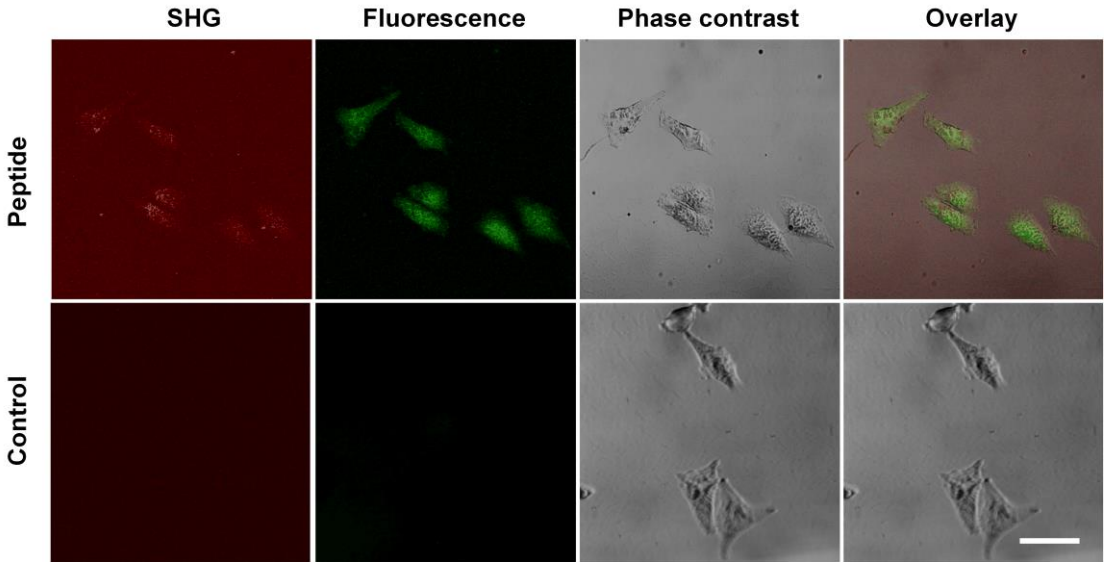

Figure 4. Cellular uptake of biotin-conjugated LK_6. Upper panel: HeLa cells exposed to biotin-conjugated LK_6 peptide containing medium. Peptides in HeLa cells displayed pseudo red color (SHG) and green color (fluorescence). Lower panel: HeLa cells exposed to normal medium without peptide (control). Scale bar: 50 μm

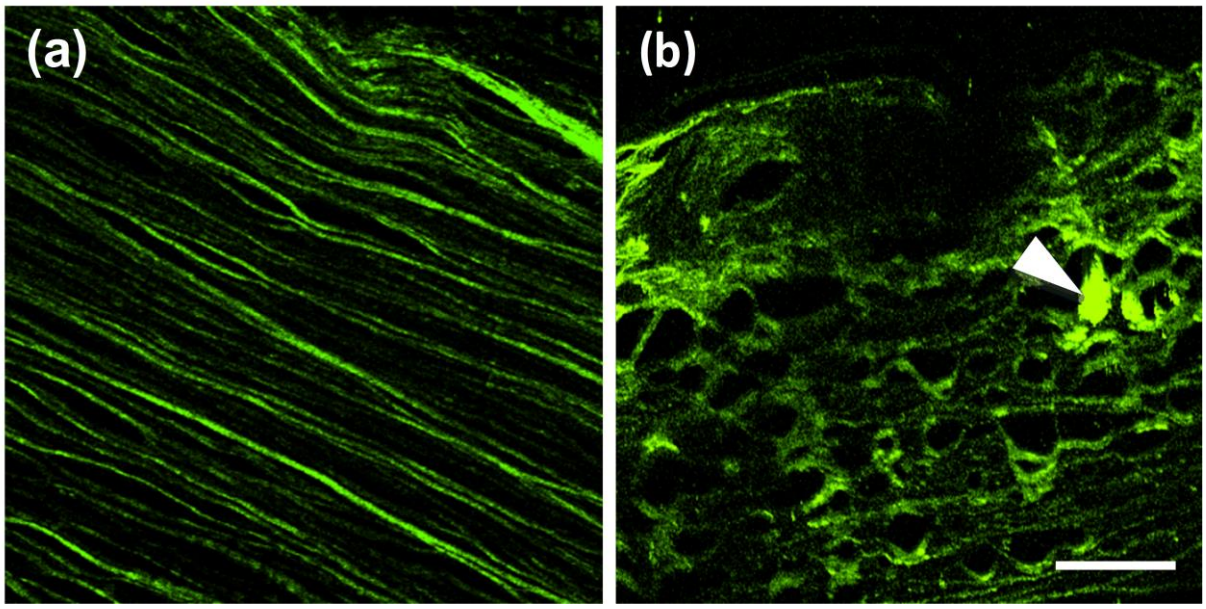

Figure 5. SHG images of human corneal biopsy samples. (a) Sample from a normal cornea (control); (b) Sample from a patient who has Lattice corneal dystrophy (LCD) disease. Collagen fibrils can be seen under SHG (green). Arrow indicates the formation of an amyloid. Scale bar: 20 μm.

Table 1. Powder SHG efficiencies of various amyloid-like peptides and human collagen subtypes.

Amyloid-like peptides / human collagens	$I^{2\omega}/I^{2\omega}$(sucrose)[a)]
IVK (IK_3)	3.31 ± 0.57
LIVAGD (LD_6)	3.06 ± 0.65
ILVAGS (IS_6)	1.96 ± 0.58
LIVAGK (LK_6)	0.95 ± 0.19
KLVFFAE (KE_7)	3.18 ± 0.67
GGVVIA (GA_6)	1.52 ± 0.43
DFNKF (DF_5)	0.89 ± 0.33
NFGAIL (NL_6)	0.76 ± 0.21
Collagen Type I	1.23 ± 0.36
Collagen Type II	0.41 ± 0.13
Collagen Type III	N.D. [b)]
Collagen Type IV	N.D. [b)]
Collagen Type V	N.D. [b)]

[a)] Value = Average ± standard deviation; [b)] N.D. = not detected.